

Nucleon Decay in a Realistic SO(10) SUSY GUT

Vincent Lucas and Stuart Raby

The Ohio State University, Department of Physics, 174 W. 18th Ave., Columbus, OH 43210

Abstract

In this paper, we calculate neutron and proton decay rates and branching ratios in a predictive SO(10) SUSY GUT which agrees well with low energy data. We show that the nucleon lifetimes are consistent with the experimental bounds. The nucleon decay rates are calculated using all one-loop chargino and gluino dressed diagrams regardless of their chiral structure. We show that the four-fermion operator $C_{jk}(u_R d_{jR})(d_{kL} \nu_{\tau L})$, commonly neglected in previous nucleon decay calculations, not only contributes significantly to nucleon decay, but, for many values of the initial GUT parameters and for large $\tan\beta$, actually dominates the decay rate. As a consequence, we find that τ_p/τ_n is often substantially larger than the prediction obtained in small $\tan\beta$ models. We also find that gluino-dressed diagrams, often neglected in nucleon decay calculations, contribute significantly to nucleon decay. In addition we find that the branching ratios obtained from this realistic SO(10) SUSY GUT differ significantly from the predictions obtained from “generic” SU(5) SUSY GUTS. Thus nucleon decay branching ratios, when observed, can be used to test theories of fermion masses.

1 Introduction

It can easily be seen that Grand Unified Theories [GUTS] contain baryon number violating operators that produce proton decay [1]. However, determining the decay rate is a much more involved task. In supersymmetric [SUSY] GUTS, the nucleon decay amplitude is directly proportional to the inverse of an effective color triplet Higgs mass \tilde{M}_t (resulting from effective dimension 5 baryon number violating operators) [2, 3] multiplied by a product of the Yukawa couplings of this color triplet Higgs to quarks and leptons. Thus, obtaining a theoretical prediction for nucleon decay rates depends critically on two factors:

1. obtaining bounds on the effective color triplet mass, and

In this regard, it has been noted that \tilde{M}_t also affects the prediction for α_s through threshold corrections at M_{GUT} . Thus, bounds on \tilde{M}_t can be obtained via the experimental constraint on α_s [4, 5, 6], but only if one has a complete SUSY GUT, valid above M_{GUT} .

2. predictions for the relevant Yukawa couplings.

The nucleon decay branching ratios are sensitive to these color triplet Higgs-quark-quark and Higgs-quark-lepton Yukawa couplings. These couplings are completely determined in any *predictive theory* of fermion masses and mixing angles, but they are typically **NOT** identical to the Yukawa couplings responsible for quark and lepton masses.

In addition, one must take these effective dimension 5 operators and renormalize them from M_{GUT} to M_Z . Then, at the weak scale, effective dimension 6 operators are obtained by closing the squark and/or slepton lines into a loop via chargino or gluino exchanges. Hence the decay rate depends sensitively on soft SUSY breaking parameters. Finally the effective dimension 6 operators are renormalized from M_Z to the nucleon mass and then an effective chiral Lagrangian analysis is used to obtain lifetimes and branching ratios.

In a recent paper [6] [paper I], we proposed several complete SO(10) SUSY GUTs, valid above M_{GUT} . At M_{GUT} , these models had the desired feature that they reproduced the effective fermion mass operators of model 4 of Anderson, et al. [7] [paper II]. Moreover, we found that if we required that our models contain in their superpotentials all terms not forbidden by the symmetries of the respective models, one and only one additional effective fermion mass operator was generated for two of the models, while no additional effective fermion mass generating operators were generated in a third model. We showed that for reasonable values of the GUT scale parameters, we can obtain values of α_s consistent with experiment, with the *effective* color triplet Higgs mass that enters into proton decay rates \tilde{M}_t as large as 10^{19} GeV or even larger. We argue, however, that the scale $\sim 10^{19}$ GeV is, in fact, a natural upper bound for \tilde{M}_t .

Note, the *actual* color triplets' masses are of order the GUT scale. Such a large value for \tilde{M}_t in comparison to the GUT scale is obtained in our model using the Dimopoulos-Wilczek mechanism for doublet-triplet splitting [8]. In Appendix 1, we review how the Dimopoulos-Wilczek mechanism can be used to obtain $\tilde{M}_t \gg M_{GUT}$.

In this paper, we present the details of our calculations of the nucleon decay rates for one of our models, referred to as model 4(c), which includes an additional “13” mass operator. In a forthcoming paper, Blažek, Carena, Wagner, and one of us (S.R.) will show that model 4(c) fits all low energy data to within 1σ , while model 4 (without the additional operator) agrees with all data at the 2σ level only [9]. Our main results for the predictions of the proton and neutron decay rates and branching ratios in model 4(c) are found in Tables A1A, A1B and A6.

In addition we have studied the sensitivity of our predictions to different factors. We have compared the predictions for our model 4(c) to those of models 4(a) through (f) of Anderson et al. This tests the sensitivity of the predicted branching ratios to the quality of the fit for fermion masses and mixing angles. We find that branching ratios can differ by factors as large as 10.

We have also compared the predictions of our models with those of small $\tan\beta$ minimal SUSY SU(5) GUTs. We find that some results in the large $\tan\beta$ regime are qualitatively different than for small $\tan\beta$. For example, certain dimension 6 operators with the chiral structure¹ LLRR tend to dominate over their LLLL counterparts for $\mu(M_Z)/m_{1/2} > 1$. In this limit, the ratio τ_p/τ_n , for example, is sensitive to the quality of the fermion mass fit and is substantially larger than what it is in small $\tan\beta$ SUSY GUTs.

Finally we discuss the sensitivity of our predictions to neglecting either the gluino or chargino exchange diagrams. We find both contributions to be significant.

The paper is organized as follows — in sections 2, 3 and 4 we discuss the calculational ingredients. Namely, in section 2, we discuss GUT models and the physics from M_{GUT} to M_Z ; in section 3, SUSY loops at M_Z and the resulting dimension 6 baryon violating operators; and in section 4, the physics from M_Z to the nucleon mass and a summary of the numerical procedure and our results. In section 5, we discuss our results and the aforementioned sensitivities to different factors.

¹ LLLL, LLRR, and RRRR refer to four-fermion operators pairing four left-handed Weyl fermions, pairing two left handed Weyl fermions and the conjugates of two right-handed Weyl fermions, and pairing the conjugates of four right-handed Weyl fermions, respectively. Specific examples of each type of four-fermion operator can be found in Table 3, *infra*.

2 The low energy effective operators generating nucleon decay, and their renormalization

Recall that in paper II, it was shown that four effective fermion mass operators, denoted \mathcal{O}_{33} , \mathcal{O}_{23} , \mathcal{O}_{12} , and \mathcal{O}_{22} , could be used to fit fermion masses and mixing angles reasonably well. For model 4 of that paper, the first three of these operators were

$$\begin{aligned}\mathcal{O}_{33} &= 16_3 10_1 16_3 \\ \mathcal{O}_{23} &= 16_2 \frac{A_2}{\tilde{A}} 10_1 \frac{A_1}{\tilde{A}} 16_3 \\ \mathcal{O}_{12} &= 16_1 \left(\frac{\tilde{A}}{\mathcal{S}_M}\right)^3 10_1 \left(\frac{\tilde{A}}{\mathcal{S}_M}\right)^3 16_2\end{aligned}$$

where 16_1 , 16_2 , and 16_3 are 16 representations containing the first, second, and third generations of fermions of the Standard Model, respectively; 10_1 is a 10 representation containing the two Higgs doublets of the Minimal Supersymmetric extension of the Standard Model; A_1 , A_2 , and \tilde{A} are 45s which get vevs in the B-L, hypercharge, and X (SU(5) invariant) directions, respectively; and \mathcal{S}_M is an SO(10) singlet getting a vev of order M_{Planck} . There were six different choices for the operator \mathcal{O}_{22} , labeled a through f.

$$\begin{aligned}\mathcal{O}_{22} = & \\ (a) & 16_2 \frac{\tilde{A}}{\mathcal{S}_M} 10_1 \frac{A_1}{\tilde{A}} 16_2 \\ (b) & 16_2 \frac{\mathcal{S}_G}{\tilde{A}} 10_1 \frac{A_1}{\mathcal{S}_M} 16_2 \\ (c) & 16_2 \frac{\tilde{A}}{\mathcal{S}_M} 10_1 \frac{A_1}{\mathcal{S}_M} 16_2 \\ (d) & 16_2 10_1 \frac{A_1}{\tilde{A}} 16_2 \\ (e) & 16_2 10_1 \frac{\tilde{A} A_1}{\mathcal{S}_M^2} 16_2 \\ (f) & 16_2 10_1 \frac{A_1 \mathcal{S}_G}{\tilde{A}^2} 16_2\end{aligned}$$

where \mathcal{S}_G is an SO(10) singlet getting a vev of order M_{GUT} . In addition, from paper I, we discovered that when we built a complete GUT, valid up to energies around M_{Planck} and we allowed all terms in the superspace potential consistent with the symmetries of the theory, an additional fermion mass generating

operator, \mathcal{O}_{13} , was generated for certain versions² of model 4.

$$\begin{aligned} \mathcal{O}_{13} = & \\ (a) \quad & 16_1 \left(\frac{\tilde{A}}{\mathcal{S}_M}\right)^3 10_1 \left(\frac{\tilde{A}A_2}{\mathcal{S}_M^2}\right) 16_3 \\ (b) \quad & 0 \\ (c) \quad & 16_1 \left(\frac{\tilde{A}}{\mathcal{S}_M}\right)^3 10_1 \left(\frac{A_2}{\mathcal{S}_M}\right) 16_3 \end{aligned}$$

At low energies, these five operators produce effective operators which generate the fermion masses and which are responsible for baryon-number violating nucleon decay.

$$\begin{aligned} & \mathcal{O}_{33} + \mathcal{O}_{23} + \mathcal{O}_{22} + \mathcal{O}_{12} + \mathcal{O}_{13} \\ & \implies \\ & H_u Q Y_u \bar{U} + H_d Q Y_d \bar{D} + H_d L Y_e \bar{E} + Q \frac{1}{2} c_{qq} Q T + Q c_{ql} L \bar{T} + \bar{U} c_{ud} \bar{D} \bar{T} + \bar{U} c_{ue} \bar{E} \bar{T} \\ & \implies \\ & H_u Q Y_u \bar{U} + H_d Q Y_d \bar{D} + H_d L Y_e \bar{E} + \frac{1}{M_t} Q \frac{1}{2} c_{qq} Q Q c_{ql} L + \frac{1}{M_t} \bar{U} c_{ud} \bar{D} \bar{U} c_{ue} \bar{E} \end{aligned}$$

with T and \bar{T} being the color triplet Higgses from 10_1 . $Y_u, Y_d, Y_e, c_{qq}, c_{ql}, c_{ud}$, and c_{ue} are flavor matrices which can be expressed in terms of seven independent real parameters. At the GUT scale, the values of these matrices are

$$\begin{aligned} Y_u &= \begin{pmatrix} 0 & C & u_u D e^{i\delta} \\ C & 0 & -\frac{1}{3} B \\ u'_u D e^{i\delta} & -\frac{4}{3} B & A \end{pmatrix} \\ Y_d &= \begin{pmatrix} 0 & -27C & u_d D e^{i\delta} \\ -27C & E e^{i\phi} & \frac{1}{9} B \\ u'_d D e^{i\delta} & -\frac{2}{9} B & A \end{pmatrix} \\ Y_e &= \begin{pmatrix} 0 & -27C & u_e D e^{i\delta} \\ -27C & 3E e^{i\phi} & B \\ u'_e D e^{i\delta} & 2B & A \end{pmatrix} \\ c_{qq} &= \begin{pmatrix} 0 & C & u_{qq} D e^{i\delta} \\ C & y_{qq} E e^{i\phi} & \frac{1}{3} B \\ u_{qq} D e^{i\delta} & \frac{1}{3} B & A \end{pmatrix} \\ c_{ql} &= \begin{pmatrix} 0 & -27C & u_{ql} D e^{i\delta} \\ -27C & y_{ql} E e^{i\phi} & \frac{1}{3} B \\ u'_{ql} D e^{i\delta} & \frac{1}{3} B & A \end{pmatrix} \end{aligned}$$

²Note, models d, e and f have the second family 16_2 coupled directly to 10_1 and a heavy 16. If this coupling is as large the third generation Yukawa coupling, then we would obtain excessively large flavor changing neutral current processes, such as $\mu \rightarrow e + \gamma$.

Table 1: y Clebsches for each version of model 4

model	y_{qq}	y_{ql}	y_{ud}	y_{ue}
a	$-3/4$	$3/4$	$-5/4$	$-3/4$
b	$-3/2$	$5/2$	$1/2$	$-3/2$
c	$-1/2$	$3/2$	$-1/2$	$-1/2$
d	$3/2$	$3/2$	$-1/2$	$3/2$
e	$1/2$	$5/2$	$1/2$	$1/2$
f	$9/4$	$3/4$	$-5/4$	$9/4$

Table 2: u Clebsches for models 4(a) through (c)

model	u_u	u'_u	u_d	u'_d	u_e	u'_e	u_{qq}	u_{ql}	u'_{ql}	u_{ud}	u'_{ud}	u_{ue}	u'_{ue}
a	$-4/3$	$1/3$	-2	-9	-54	3	$1/3$	3	-9	-2	36	2	$-4/3$
b	0	0	0	0	0	0	0	0	0	0	0	0	0
c	$-4/3$	$1/3$	$2/3$	-9	-54	-1	$1/3$	-1	-9	$2/3$	36	2	$-4/3$

$$\begin{aligned}
c_{ud} &= \begin{pmatrix} 0 & -27C & u_{ud}De^{i\delta} \\ -27C & y_{ud}Ee^{i\phi} & -\frac{4}{9}B \\ u'_{ud}De^{i\delta} & \frac{2}{9}B & A \end{pmatrix} \\
c_{ue} &= \begin{pmatrix} 0 & C & u_{ue}De^{i\delta} \\ C & y_{ue}Ee^{i\phi} & -4B \\ u'_{ue}De^{i\delta} & -2B & A \end{pmatrix} \quad (1)
\end{aligned}$$

with the values of the Clebsches given in Tables 1 and 2.

These matrices need to be renormalized from the GUT scale to the electroweak scale. Due to the no-renormalization theorems of supersymmetry, only wavefunction renormalizations enter into the calculation of the renormalization group equations of these matrices. The RGEs for the matrices are

$$\begin{aligned}
\frac{dc_{qq}}{dt} &= \frac{1}{16\pi^2} [(Y_u Y_u^\dagger + Y_d Y_d^\dagger)c_{qq} + c_{qq}(Y_u Y_u^\dagger + Y_d Y_d^\dagger)^T \\
&\quad - (\frac{16}{3}g_3^2 + 3g_2^2 + \frac{1}{15}g_1^2)c_{qq}] \\
\frac{dc_{ql}}{dt} &= \frac{1}{16\pi^2} [(Y_u Y_u^\dagger + Y_d Y_d^\dagger)c_{ql} + c_{ql}(Y_e Y_e^\dagger)^T \\
&\quad - (\frac{8}{3}g_3^2 + 3g_2^2 + \frac{1}{3}g_1^2)c_{ql}] \quad (2)
\end{aligned}$$

$$\begin{aligned}\frac{dc_{ud}}{dt} &= \frac{1}{16\pi^2} [2(Y_u^\dagger Y_u)^T c_{ud} + 2c_{ud} Y_d^\dagger Y_d - (\frac{16}{3}g_3^2 + \frac{2}{3}g_1^2)c_{ud}] \\ \frac{dc_{ue}}{dt} &= \frac{1}{16\pi^2} [2(Y_u^\dagger Y_u)^T c_{ue} + 2c_{ue} Y_e^\dagger Y_e - (\frac{8}{3}g_3^2 + \frac{26}{15}g_1^2)c_{ue}]\end{aligned}$$

with $t = \log(\mu/M_Z)$.

3 Nucleon decay formulas

At low energies, the matrices Y_u , Y_d , and Y_e are diagonalized by unitary matrices called S and T defined so that

$$S_u Y_u T_u = \begin{pmatrix} \lambda_u & & \\ & \lambda_c & \\ & & \lambda_t \end{pmatrix} \equiv \hat{Y}_u,$$

and so forth, with all diagonal entries in \hat{Y}_u , \hat{Y}_d , and \hat{Y}_e being real and positive. The weak eigenstate basis for the fermionic fields will be represented by primed fields, and the mass eigenstate basis will be represented by unprimed letters. Additionally, we choose an unprimed basis for neutrinos such that

$$S_e^* \nu' = \nu,$$

so that the lepton-lepton-weak boson vertices are flavor diagonal in the unprimed basis.³

Squarks and sleptons mass matrices are diagonalized using 6 by 6 matrices Γ defined

$$\Gamma_\Omega \left(\begin{array}{c|c} S_\Omega^* & \\ \hline & T_\Omega^T \end{array} \right) \begin{pmatrix} \tilde{\Omega}' \\ \tilde{\Omega}'^* \end{pmatrix} = \tilde{\Omega}, \quad \Omega = u, d, e$$

where $\tilde{\Omega}$ is a six dimensional vector of mass eigenstates and $\tilde{\Omega}'$ and $\tilde{\Omega}'^*$ are weak eigenstates. Cf. notation of [10]. Additionally, we define $\Gamma_{\Omega,L}$ and $\Gamma_{\Omega,R}$ to be 6 by 3 matrices so that $\Gamma_{\Omega,L}$ consists of the first three columns of Γ_Ω and $\Gamma_{\Omega,R}$ consists of the last three columns. In block matrix notation,

$$\Gamma_\Omega = (\Gamma_{\Omega,L} \mid \Gamma_{\Omega,R})$$

Since there is no left-handed right-handed neutrino mixing, we will define Γ_ν so that

$$\Gamma_\nu S_e^* \tilde{\nu}' = \tilde{\nu}$$

³If left-handed neutrinos have a mass, the ν_e , ν_μ , and ν_τ thus defined are generally not mass eigenstates. Since we sum decay rates over all neutrino species in our analysis, the convention for defining the neutrino basis is irrelevant for our results. In paper I, the 3 left-handed neutrinos remain massless, but this result is easily changed with the introduction of GUT scale majorana neutrino masses for heavy singlet neutrinos.

with $\tilde{\nu}$ being a mass eigenstate basis for the sneutrinos. A right-handed Γ_ν matrix will not be defined.

Finally, the chargino mass matrices are diagonalized by matrices U_+ and U_- defined

$$\begin{pmatrix} \tilde{W}_+ \\ \tilde{H}_+ \end{pmatrix} = U_+ \begin{pmatrix} \tilde{\chi}_1^+ \\ \tilde{\chi}_2^+ \end{pmatrix}$$

and

$$\begin{pmatrix} \tilde{W}_- \\ \tilde{H}_- \end{pmatrix} = U_- \begin{pmatrix} \tilde{\chi}_1^- \\ \tilde{\chi}_2^- \end{pmatrix}$$

where $\tilde{\chi}_{1,2}^\pm$ are mass eigenstates.

In this notation, various Feynman vertices relevant to nucleon decay are given in Appendix 2.

3.1 Gluino diagrams

Figure 1 shows the two diagrams which contribute to the four-fermion operator $C_{ijkl}^{(ud)(d\nu)[G]}(u_i^\alpha d_j^\beta)(d_k^\gamma \nu_l)\epsilon_{\alpha\beta\gamma}$. Calculating these two diagrams, we find

$$C_{ijkl}^{(ud)(d\nu)[G]} = \frac{4}{3} \frac{1}{16\pi^2 \tilde{M}_t} g_3^2 \left\{ \Gamma_{U,L \lambda i} \Gamma_{U,L \lambda i'}^* \Gamma_{D,L \rho j} \Gamma_{D,L \rho j'}^* \hat{c}_{qq}^{i' [j' \hat{c}_{ql}^{k] l}]} m_{\tilde{g}} I(\tilde{g}, \tilde{u}_\lambda, \tilde{d}_\rho) - \Gamma_{D,L \rho j} \Gamma_{D,L \rho j'}^* \Gamma_{D,L \sigma k} \Gamma_{D,L \sigma k'}^* \hat{c}_{qq}^{i [j' \hat{c}_{ql}^{k'] l}]} m_{\tilde{g}} I(\tilde{g}, \tilde{d}_\rho, \tilde{d}_\sigma) \right\}$$

where $\alpha, \beta,$ and γ are color indices, $i, i', j, j', k,$ and l are fermion flavor indices, ρ and λ are squark flavor indices, $\hat{c}_{qq} = S_u c_{qq}^R S_d^T$, $\hat{c}_{ql} = S_d c_{ql}^R S_e^T$ with c_{qq}^R and c_{ql}^R being c_{qq} and c_{ql} , respectively, renormalized to M_Z , and

$$I(a, b, c) = \frac{m_a^2 \log m_a^2}{(m_a^2 - m_b^2)(m_a^2 - m_c^2)} + \frac{m_b^2 \log m_b^2}{(m_b^2 - m_c^2)(m_b^2 - m_a^2)} + \frac{m_c^2 \log m_c^2}{(m_c^2 - m_a^2)(m_c^2 - m_b^2)}$$

where m_a equals the mass of particle a , etc.⁴

By similar calculations, we can construct the remaining four-fermion operators listed in Table 3. Note, we also use Table 3 to define our notation for these four-fermion operators. The C_{ijkl} s for these operators are

$$C_{ijkl}^{(ud)(ue)[G]} = -\frac{4}{3} \frac{1}{16\pi^2 \tilde{M}_t} g_3^2 \left\{ \Gamma_{U,L \lambda i} \Gamma_{U,L \lambda i'}^* \Gamma_{D,L \rho j} \Gamma_{D,L \rho j'}^* \hat{c}_{qq}^{[i' j' \check{c}_{ql}^{k] l}]} m_{\tilde{g}} I(\tilde{g}, \tilde{u}_\lambda, \tilde{d}_\rho) - \Gamma_{U,L \lambda i} \Gamma_{U,L \lambda i'}^* \Gamma_{U,L \sigma k} \Gamma_{U,L \sigma k'}^* \hat{c}_{qq}^{[i' j' \check{c}_{ql}^{k'] l}]} m_{\tilde{g}} I(\tilde{g}, \tilde{u}_\lambda, \tilde{u}_\sigma) \right\}$$

$$C_{ijkl}^{(\bar{d}\bar{d})(u\nu)[G]} = \frac{4}{3} \frac{1}{16\pi^2 \tilde{M}_t} g_3^2 \Gamma_{D,R \rho j} \Gamma_{D,L \rho j'}^* \Gamma_{D,R \sigma k} \Gamma_{D,L \sigma k'}^* \hat{c}_{qq}^{i [j' \hat{c}_{ql}^{k'] l}]} m_{\tilde{g}} I(\tilde{g}, \tilde{d}_\rho, \tilde{d}_\sigma)$$

⁴We use a notation for antisymmetrization on tensor indices in which $A_{i[jkl]mn}$ is equal to $A_{ijklmn} - A_{ilkjmn}$, and so forth.

Figure 1:

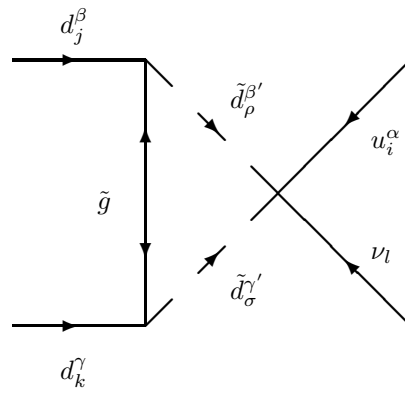
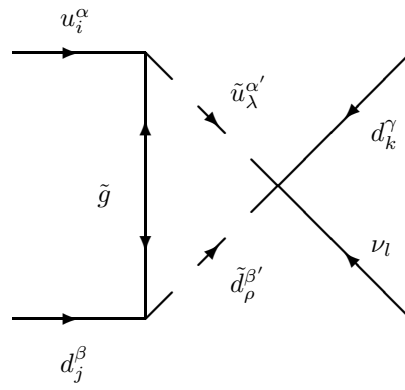


Table 3: Table of all gluino-dressed four fermion operators relevant to nucleon decay

operator type		
LLLL	LLRR	RRRR
$C_{ijkl}^{(ud)(d\nu)[G]}(u_i^\alpha d_j^\beta)(d_k^\gamma \nu_l)\epsilon_{\alpha\beta\gamma}$	$C_{ijkl}^{(dd)(u\nu)[G]}(\overline{d_j^{*\beta}} \overline{d_k^{*\gamma}})(u_i^\alpha \nu_l)\epsilon_{\alpha\beta\gamma}$ $C_{ijkl}^{(ud)(d\nu)[G]}(\overline{u_i^{*\alpha}} \overline{d_j^{*\beta}})(d_k^\gamma \nu_l)\epsilon_{\alpha\beta\gamma}$	
$C_{ijkl}^{(ud)(ue)[G]}(u_i^\alpha d_j^\beta)(u_k^\gamma e_l)\epsilon_{\alpha\beta\gamma}$	$C_{ijkl}^{(ud)(ue)[G]}(\overline{u_i^{*\alpha}} \overline{d_j^{*\beta}})(u_k^\gamma e_l)\epsilon_{\alpha\beta\gamma}$ $C_{ijkl}^{(ud)(\overline{ue})[G]}(u_i^\alpha d_j^\beta)(\overline{u_k^{*\gamma}} \overline{e_l^{*\delta}})\epsilon_{\alpha\beta\gamma}$	$C_{ijkl}^{(ud)(ue)[G]}(\overline{u_i^{*\alpha}} \overline{d_j^{*\beta}})(\overline{u_k^{*\gamma}} \overline{e_l^{*\delta}})\epsilon_{\alpha\beta\gamma}$

$$\begin{aligned}
C_{ijkl}^{(\overline{ud})(d\nu)[G]} &= \frac{4}{3} \frac{1}{16\pi^2 \tilde{M}_t} g_3^2 \Gamma_{U,R} \lambda_i \Gamma_{U,L}^* \lambda_{i'} \Gamma_{D,R} \rho_j \Gamma_{D,L}^* \rho_{j'} \hat{c}_{qq}^{i'j'} \hat{c}_{ql}^{kl} m_{\tilde{g}} I(\tilde{g}, \tilde{u}_\lambda, \tilde{d}_\rho) \\
C_{ijkl}^{(\overline{ud})(ue)[G]} &= -\frac{4}{3} \frac{1}{16\pi^2 \tilde{M}_t} g_3^2 \Gamma_{U,R} \lambda_i \Gamma_{U,L}^* \lambda_{i'} \Gamma_{D,R} \rho_j \Gamma_{D,L}^* \rho_{j'} \hat{c}_{qq}^{[i'j']} \check{c}_{ql}^{kl} m_{\tilde{g}} I(\tilde{g}, \tilde{u}_\lambda, \tilde{d}_\rho) \\
C_{ijkl}^{(ud)(\overline{ue})[G]} &= -\frac{4}{3} \frac{1}{16\pi^2 \tilde{M}_t} g_3^2 \Gamma_{U,L} \lambda_i \Gamma_{U,R}^* \lambda_{i'} \Gamma_{D,L} \rho_j \Gamma_{D,R}^* \rho_{j'} \hat{c}_{ud}^{[i'j']} \hat{c}_{ue}^{kl} m_{\tilde{g}} I(\tilde{g}, \tilde{u}_\lambda, \tilde{d}_\rho) \\
C_{ijkl}^{(\overline{ud})(\overline{ue})[G]} &= -\frac{4}{3} \frac{1}{16\pi^2 \tilde{M}_t} g_3^2 \{ \Gamma_{U,R} \lambda_i \Gamma_{U,R}^* \lambda_{i'} \Gamma_{D,R} \rho_j \Gamma_{D,R}^* \rho_{j'} \hat{c}_{ud}^{[i'j']} \hat{c}_{ue}^{kl} m_{\tilde{g}} I(\tilde{g}, \tilde{u}_\lambda, \tilde{d}_\rho) - \\
&\quad \Gamma_{U,R} \lambda_i \Gamma_{U,R}^* \lambda_{i'} \Gamma_{U,R} \sigma_k \Gamma_{U,R}^* \sigma_{k'} \hat{c}_{ud}^{[i'j]} \hat{c}_{ue}^{k'l} m_{\tilde{g}} I(\tilde{g}, \tilde{u}_\lambda, \tilde{u}_\sigma) \}
\end{aligned}$$

where $\check{c}_{ql} = S_u c_{ql}^R S_e^T$, $\hat{c}_{ud} = T_u^T c_{ud}^R T_d$, and $\hat{c}_{ue} = T_u^T c_{ue}^R T_e$ with c_{ud}^R and c_{ue}^R being c_{ud} and c_{ue} , respectively, renormalized to M_Z .

As observed in ref. [11], the contribution of gluino dressed operators is zero in the limit that all squarks are degenerate at the electroweak scale. In this analysis, however, squarks and sleptons are assumed degenerate at M_{GUT} and as a consequence of renormalization group running they are explicitly non-degenerate at the weak scale. Thus we retain the gluino contribution in our analysis.

In principle, we could also have four-fermion operators like $C_{ijkl}^{(\overline{uu})(de)[G]} \times (\overline{u_i^{*\alpha}} \overline{u_k^{*\gamma}})(d_j^\beta e_l)\epsilon_{\alpha\beta\gamma}$ pairing two up type quarks in a Weyl index contracted pair. However, since we are only interested in the first generation of up quarks, the portions of these operators that would be relevant to nucleon decay are identically zero.

3.2 Chargino diagrams

Using the vertices in Appendix 2, the chargino diagrams can be readily computed. According to analyses by many other authors on proton decay in SUSY GUTs, the dominant operators would be expected to be $C_{ijkl}^{(ud)(d\nu)[W]}(u_i^\alpha d_j^\beta)(d_k^\gamma \nu_l)\epsilon_{\alpha\beta\gamma}$ and $C_{ijkl}^{(ud)(ue)[W]}(u_i^\alpha d_j^\beta)(u_k^\gamma e_l)\epsilon_{\alpha\beta\gamma}$. The C_{ijkl} s for these operators are equal to

$$C_{ijkl}^{(ud)(d\nu)[W]} = \frac{1}{16\pi^2 \tilde{M}_t} \left\{ [(g_2 \Gamma_{D,L} U_{-1n} - \Gamma_{D,R} \hat{Y}_d U_{-2n}) V_{KM}^\dagger]_{\rho i} \right. \\ \times [(g_2 \Gamma_{U,L} U_{+1n} - \Gamma_{U,R} \hat{Y}_u U_{+2n}) V_{KM}]_{\lambda j} \\ \times \Gamma_{U,L}^* \lambda i' \Gamma_{D,L}^* \rho j' \hat{c}_{qq}^{i' [j' \hat{c}_{ql}^{k}] l} m_{\tilde{\chi}_n} I(\tilde{\chi}_n, \tilde{u}_\lambda, \tilde{d}_\rho) \\ + [(g_2 \Gamma_{U,L} U_{+1n} - \Gamma_{U,R} \hat{Y}_u U_{+2n}) V_{KM}]_{\lambda k} \\ \times [(g_2 \Gamma_{E,L} U_{-1n} - \Gamma_{E,R} \hat{Y}_e U_{-2n})]_{\rho l} \\ \left. \times \Gamma_{U,L}^* \lambda k' \Gamma_{E,L}^* \rho l' \hat{c}_{qq}^{[ij \hat{c}_{ql}^{k'}] l'} m_{\tilde{\chi}_n} I(\tilde{\chi}_n, \tilde{u}_\lambda, \tilde{e}_\rho) \right\}$$

$$C_{ijkl}^{(ud)(ue)[W]} = -\frac{1}{16\pi^2 \tilde{M}_t} \left\{ [(g_2 \Gamma_{D,L} U_{-1n} - \Gamma_{D,R} \hat{Y}_d U_{-2n}) V_{KM}^\dagger]_{\rho i} \right. \\ \times [(g_2 \Gamma_{U,L} U_{+1n} - \Gamma_{U,R} \hat{Y}_u U_{+2n}) V_{KM}]_{\lambda j} \\ \times \Gamma_{U,L}^* \lambda i' \Gamma_{D,L}^* \rho j' \hat{c}_{qq}^{[i' j' \hat{c}_{ql}^{k}] l} m_{\tilde{\chi}_n} I(\tilde{\chi}_n, \tilde{u}_\lambda, \tilde{d}_\rho) \\ + [(g_2 \Gamma_{D,L} U_{-1n} - \Gamma_{D,R} \hat{Y}_d U_{-2n}) V_{KM}^\dagger]_{\rho k} \\ \times g_2 \Gamma_{\nu \lambda l} U_{+1n} \Gamma_{D,L}^* \rho k' \Gamma_{\nu \lambda l'} \hat{c}_{qq}^{[j \hat{c}_{ql}^{k'}] l'} m_{\tilde{\chi}_n} I(\tilde{\chi}_n, \tilde{d}_\rho, \tilde{\nu}_\lambda) \left. \right\}$$

The C_{ijkl} s for the LLRR and RRRR operators are

$$C_{ijkl}^{(\overline{ud})(d\nu)[W]} = \frac{1}{16\pi^2 \tilde{M}_t} \left\{ U_{+2n}^* (\Gamma_{D,L} V_{KM}^\dagger \hat{Y}_u)_{\rho i} U_{-2n}^* (\Gamma_{U,L} V_{KM} \hat{Y}_d)_{\lambda j} \right. \\ \times \Gamma_{U,L}^* \lambda i' \Gamma_{D,L}^* \rho j' \hat{c}_{qq}^{i' [j' \hat{c}_{ql}^{k}] l} m_{\tilde{\chi}_n} I(\tilde{\chi}_n, \tilde{u}_\lambda, \tilde{d}_\rho) \\ + [(g_2 \Gamma_{U,L} U_{+1n} - \Gamma_{U,R} \hat{Y}_u U_{+2n}) V_{KM}]_{\lambda k} \\ \times [(g_2 \Gamma_{E,L} U_{-1n} - \Gamma_{E,R} \hat{Y}_e U_{-2n})]_{\rho l} \\ \left. \times \Gamma_{U,R}^* \lambda k' \Gamma_{E,R}^* \rho l' \hat{c}_{ud}^{[ij \hat{c}_{ue}^{k'}] l'} m_{\tilde{\chi}_n} I(\tilde{\chi}_n, \tilde{u}_\lambda, \tilde{e}_\rho) \right\}$$

$$C_{ijkl}^{(ud)(\overline{ue})[W]} = -\frac{1}{16\pi^2 \tilde{M}_t} \left\{ [(g_2 \Gamma_{D,L} U_{-1n} - \Gamma_{D,R} \hat{Y}_d U_{-2n}) V_{KM}^\dagger]_{\rho i} \right.$$

$$\begin{aligned}
& \times [(g_2 \Gamma_{U,L} U_{+1n} - \Gamma_{U,R} \hat{Y}_u U_{+2n}) V_{KM}]_{\lambda j} \\
& \times \Gamma_{U,R}^* \lambda i' \Gamma_{D,R}^* \rho j' \hat{c}_{ud}^{* [i' j' \hat{c}_{ue}^* k] l} m_{\tilde{\chi}_n} I(\tilde{\chi}_n, \tilde{u}_\lambda, \tilde{d}_\rho) \\
& + U_{+2n}^* (\Gamma_{D,L} V_{KM}^\dagger \hat{Y}_u)_{\rho k} U_{-2n}^* (\Gamma_\nu \hat{Y}_e)_{\lambda l} \\
& \times \Gamma_{D,L}^* \rho k' \Gamma_\nu^* \lambda l' \hat{c}_{qq}^{* [i j \hat{c}_{ql}^{* k} l' m_{\tilde{\chi}_n} I(\tilde{\chi}_n, \tilde{d}_\rho, \tilde{\nu}_\lambda) \}}
\end{aligned}$$

$$\begin{aligned}
C_{ijkl}^{(\overline{ud})(ue)[W]} &= -\frac{1}{16\pi^2 \tilde{M}_t} \left\{ U_{+2n}^* (\Gamma_{D,L} V_{KM}^\dagger \hat{Y}_u)_{\rho i} U_{-2n}^* (\Gamma_{U,L} V_{KM} \hat{Y}_d)_{\lambda j} \right. \\
& \left. \times \Gamma_{U,L}^* \lambda i' \Gamma_{D,L}^* \rho j' \hat{c}_{qq}^{* [i' j' \hat{c}_{ql}^{* k] l} m_{\tilde{\chi}_n} I(\tilde{\chi}_n, \tilde{u}_\lambda, \tilde{d}_\rho) \right\}
\end{aligned}$$

$$\begin{aligned}
C_{ijkl}^{(\overline{ud})(\overline{ue})[W]} &= -\frac{1}{16\pi^2 \tilde{M}_t} \left\{ U_{+2n}^* (\Gamma_{D,L} V_{KM}^\dagger \hat{Y}_u)_{\rho i} U_{-2n}^* (\Gamma_{U,L} V_{KM} \hat{Y}_d)_{\lambda j} \right. \\
& \left. \times \Gamma_{U,R}^* \lambda i' \Gamma_{D,R}^* \rho j' \hat{c}_{ud}^{* [i' j' \hat{c}_{ue}^* k] l} m_{\tilde{\chi}_n} I(\tilde{\chi}_n, \tilde{u}_\lambda, \tilde{d}_\rho) \right\}
\end{aligned}$$

4 Numerical procedure and results

In calculating the following nucleon decay rates, we make the standard universal-ity assumptions about the soft SUSY parameters at M_{GUT} , except that we allow non-universal values for M_{H_u} and M_{H_d} .⁵ We define M_{GUT} such that $\alpha_1 = \alpha_2 \equiv \tilde{\alpha}_{GUT}$ at M_{GUT} and define ϵ_3 , representing the contribution of GUT scale threshold corrections to the gauge couplings, to be $(\alpha_3(M_{GUT}) - \tilde{\alpha}_{GUT})/\tilde{\alpha}_{GUT}$. The dimensionless (dimensionful) parameters are renormalized at two (one) loops to M_Z using the renormalization group equations of Martin and Vaughn [12], except that c_{qq} , c_{ql} , c_{ud} , and c_{ue} are renormalized at one loop using the equations of this paper.

Renormalization of the C_{ijkl} s from M_Z to 1 GeV is taken into account by multiplying them by the A_L calculated in [13], and then chiral Lagrangian

⁵Note that if the messenger scale of SUSY breaking is M_{Planck} then our analysis is not completely self-consistent. In any complete SUSY GUT defined up to an effective cut-off scale $M > M_G$, the interactions above M_G will renormalize the soft breaking parameters. This will, in general, split the degeneracy of squark and slepton masses at M_G even if they are degenerate at M . On the other hand, bounds on flavor changing neutral current processes, severely constrain the magnitude of possible splitting. Thus these corrections must be small. In addition, in theories where SUSY breaking is mediated by gauge exchanges with a messenger scale below (but near) M_G , the present analysis is expected to apply unchanged. Since in this case squarks and sleptons will be nearly degenerate at the messenger scale. The Higgs masses, on the other hand, are probably dominated by new interactions which also generate a μ term. It is thus plausible to expect the Higgs masses to be split and independent of squark and slepton masses. The parameter A_0 could also be universal at the messenger scale.

techniques [14] are used to obtain nucleon decay amplitudes. Formulas for nucleon decay rates in terms of the chiral Lagrangian parameters are contained in Appendix 3.

The decay rates depend heavily on the chiral Lagrangian factors α and β where

$$\beta U(\mathbf{k}) = \epsilon_{\alpha\beta\gamma} \langle 0 | (u^\alpha d^\beta) u^\gamma | \text{proton}(\mathbf{k}) \rangle,$$

$$\alpha U(\mathbf{k}) = \epsilon_{\alpha\beta\gamma} \langle 0 | (\bar{u}^* \alpha \bar{d}^* \beta) u^\gamma | \text{proton}(\mathbf{k}) \rangle$$

and $U(\mathbf{k})$ is the left handed component of the proton's wavefunction. See, e.g., ref. [15]. It is known that $|\beta| = |\alpha|$ [15, 16] and that $|\beta|$ ranges from .003 to .03 GeV^3 [17]. Lattice calculations have not reduced the uncertainty in $|\beta|$; lattice calculations have reported $|\beta|$ as low as .006 GeV^3 [16] and as high as .03 GeV^3 [18]. Additionally, the phase between α and β is not widely reported, although a relatively recent lattice calculation suggests that $\beta = -\alpha$ [16]. Therefore, we have left the phase between α and β a free variable, and report three values for many of the quantities predicted in our tables. Namely, the max (min) referred to in the tables is the value for the quantity predicted when the phase between α and β is such that the quantity is maximized (minimized). Hence, each entry in the max and min columns uses a different value of $\arg(\beta/\alpha)$.

In the following tables, we have calculated decay rates using $\tilde{M}_t = 10^{19}$ GeV and $|\beta| = .003$ GeV^3 . In paper I, we showed that without any fine tuning this value of \tilde{M}_t can be made consistent with the measured value for α_s . In addition, we argued that it seems unnatural to have \tilde{M}_t much bigger than 10^{19} GeV in the sense that in order to have \tilde{M}_t much bigger than 10^{19} GeV, there would need to be a supermassive electroweak doublet in the GUT desert with mass many orders of magnitude lower than the GUT scale itself and at least an order of magnitude lighter than any other particle getting mass around the GUT scale. Therefore, the values presented in the tables are roughly upper bounds on the nucleons' lifetimes, based on naturalness⁶. Since all decay rates scale as $(\frac{|\beta|}{.003 \text{ GeV}^3} \frac{10^{19} \text{ GeV}}{\tilde{M}_t})^2$, the lifetimes for different values of \tilde{M}_t and $|\beta|$ can easily be extracted from the tables.

In Tables A1 through A6 [the A tables], we calculate nucleon decay using model 4(c) (including the \mathcal{O}_{13} operator of paper I), since it appears to be the model which best fits the low energy data [9]. Initial values for the dimensionless Yukawa parameters; soft SUSY parameters; and M_{GUT} , $\tilde{\alpha}_{GUT}$, and $\tan\beta$ are taken from the global χ^2 analysis of Blažek et al. [9]. This global χ^2 analysis shows that these values of the GUT parameters are consistent with electroweak

⁶A note of caution – it was also shown in ref. [16] that chiral Lagrangian techniques overestimate the amplitude $\epsilon_{\alpha\beta\gamma} \langle \pi^0 | (u^\alpha d^\beta) u^\gamma | p \rangle$ by at least a factor of 2.4 (for $\beta = 0.006$). Thus the proton decay rate is overestimated by almost a factor of 6 or more in this case. As a result, for any given $|\beta|$, the actual nucleon lifetimes for that β , could be a factor of 6 or more larger than the results reported here, as extrapolated from our tables for that value of $|\beta|$. These remarks are indicative of the theoretical uncertainty in the calculation due to strong interaction effects.

symmetry breaking and the experimental bounds on the sparticle masses; and that, for the particular values of the soft SUSY breaking parameters used, these parameters give the best global fit to 20 low energy observables, including experimental measurements for the gauge couplings; fermion masses and mixing angles; and $b \rightarrow s\gamma$, with χ^2 per degree of freedom $< 1\frac{1}{3}$. Tables A1A and A1B contain the lifetimes for $p \rightarrow K^+\bar{\nu}$ and $n \rightarrow K^0\bar{\nu}$ and compares these rates with the rates of decay into the other significant decay modes involving spin zero mesons, for various values of the GUT scale parameters. These are the main results of this paper. Note however that only the three or four most significant decay modes are included in these tables.

In the subsequent tables we evaluate the relative contributions to these rates from different sources – (LLRR vs. LLLL operators) or (gluinos vs. charginos). Tables A2A, A2B, A3A, and A3B compare the contributions of chargino and gluino diagrams to the total decay rate. Table A4 compares the contribution of LLLL versus LLRR operators for decays into anti-neutrinos, for each of the three anti-neutrino species. Tables A5A and A5B compare the relative importance of each generation of anti-neutrino to the total proton decay rate, for decay modes involving anti-neutrinos. Finally, Table A6 contains the values of the GUT scale parameters used in Tables A1 through A5.

Tables B1 through B6 [the B tables] contain information similar to that in the A tables except that they compare models 4(a) through (f), without the \mathcal{O}_{13} operator. We used values for the initial (GUT scale) parameters, taken from unreported data from the collaboration of ref. [9], which are consistent with electroweak symmetry breaking and the experimental bounds on sparticle masses, and which give predictions agreeing to within 2.1σ with experimental measurements for gauge couplings, fermion masses and mixing angles, and $b \rightarrow s\gamma$. This comparison gives us information on the model dependence of nucleon decay branching ratios. Note that models 4(a) through (f) (without the \mathcal{O}_{13} operator) give identical results for fermion masses and mixing angles. This is because the contribution of the different \mathcal{O}_{22} operators to the 22 entry of the Yukawa matrices all give the same Clebsch relation 0:1:3 for u:d:e matrices [7]. They however have different Clebsch relations for the 22 entry of the matrices c_{qq} , c_{ql} , c_{ud} , and c_{ue} relevant for nucleon decay.

In addition, the comparison of model 4(c), with the \mathcal{O}_{13} operator, to models 4(a) through (f), without the \mathcal{O}_{13} operator, gives us information on the sensitivity of predictions for nucleon decay with respect to the quality of the fit for fermion masses and mixing angles. In order to compare the runs in the A tables directly with the runs in the B tables, we chose the GUT scale parameters such that for each run in the B tables, the values for $\tilde{\alpha}_{GUT}^{-1}$, M_{GUT} , ϵ_3 ; the soft SUSY breaking parameters $\tan\beta$, μ , $m_{1/2}$, m_0 , m_{H_u} , m_{H_d} , and A_0 ; and the Yukawa parameter A are nearly the same as they are for the run of the same name in the A tables.

run no.	$\tau(p \rightarrow K^+\bar{\nu})/(10^{32}\text{yrs})$			$\frac{\Gamma(p \rightarrow \pi^+\bar{\nu})}{\Gamma(p \rightarrow K^+\bar{\nu})}$			$\frac{\Gamma(p \rightarrow K^0\mu^+)}{\Gamma(p \rightarrow K^+\bar{\nu})} \times 10^2$			$\frac{\Gamma(p \rightarrow \pi^0\mu^+)}{\Gamma(p \rightarrow K^+\bar{\nu})} \times 10^2$			$\frac{\Gamma(p \rightarrow \eta\mu^+)}{\Gamma(p \rightarrow K^+\bar{\nu})} \times 10^2$		
	max	$\beta = -\alpha$	min	max	$\beta = -\alpha$	min	max	$\beta = -\alpha$	min	max	$\beta = -\alpha$	min	max	$\beta = -\alpha$	min
I	26.	14.	14.	0.46	0.39	0.39	0.52	0.29	0.29	0.28	0.16	0.16	0.099	0.055	0.055
II	60.	37.	37.	0.37	0.33	0.32	0.53	0.33	0.32	0.29	0.18	0.18	0.10	0.062	0.061
III(1)	220.	130.	98.	1.1	0.74	0.69	0.31	0.19	0.14	0.12	0.073	0.055	0.028	0.017	0.013
III(2)	150.	97.	74.	1.5	1.1	0.94	0.37	0.24	0.18	0.11	0.071	0.054	0.017	0.011	0.0084
III(3)	110.	76.	58.	1.5	1.1	1.0	0.34	0.23	0.18	0.092	0.063	0.049	0.011	0.0078	0.0060

Table A1A: Partial mean lifetime for proton decaying into kaon plus anti-neutrino and ratios of the rates of proton decay into various decay products versus rate of decay into kaon plus anti-neutrino for various values of the GUT scale parameters, when the \mathcal{O}_{13} operator is included.

run no.	$\tau(n \rightarrow K^0\bar{\nu})/(10^{32}\text{yrs})$			$\frac{\Gamma(n \rightarrow \pi^0\bar{\nu})}{\Gamma(n \rightarrow K^0\bar{\nu})} \times 10^2$			$\frac{\Gamma(n \rightarrow \eta\bar{\nu})}{\Gamma(n \rightarrow K^0\bar{\nu})} \times 10^2$			$\frac{\Gamma(n \rightarrow \pi^-\mu^+)}{\Gamma(n \rightarrow K^0\bar{\nu})} \times 10^2$		
	max	$\beta = -\alpha$	min	max	$\beta = -\alpha$	min	max	$\beta = -\alpha$	min	max	$\beta = -\alpha$	min
I	3.8	2.3	2.3	3.3	3.2	3.2	0.37	0.17	0.17	0.083	0.051	0.050
II	12.	7.3	6.9	3.3	3.2	3.2	0.49	0.25	0.23	0.11	0.070	0.067
III(1)	14.	12.	9.8	3.5	3.5	3.4	0.13	0.088	0.035	0.016	0.014	0.011
III(2)	6.4	5.8	5.0	3.2	3.1	3.1	0.079	0.055	0.022	0.0094	0.0085	0.0073
III(3)	4.5	4.2	3.7	3.2	3.1	3.1	0.063	0.045	0.019	0.0076	0.0070	0.0061

Table A1B: Partial mean lifetime for neutron decaying into kaon plus anti-neutrino and ratios of the rates of proton decay into various decay products versus rate of decay into kaon plus anti-neutrino for various values of the GUT scale parameters, when the \mathcal{O}_{13} operator is included.

run no.	$\frac{\Gamma_{p \rightarrow K^+\bar{\nu}}^{\text{chargino}}}{\Gamma_{p \rightarrow K^+\bar{\nu}}^{\text{total}}}$			$\frac{\Gamma_{p \rightarrow \pi^+\bar{\nu}}^{\text{chargino}}}{\Gamma_{p \rightarrow \pi^+\bar{\nu}}^{\text{total}}}$			$\frac{\Gamma_{p \rightarrow K^0\mu^+}^{\text{chargino}}}{\Gamma_{p \rightarrow K^0\mu^+}^{\text{total}}}$		
	max	$\beta = -\alpha$	min	max	$\beta = -\alpha$	min	max	$\beta = -\alpha$	min
I	1.1	1.1	0.90	1.1	1.1	0.87	0.99	0.99	0.99
II	1.3	1.2	0.82	1.3	1.2	0.73	1.0	1.0	1.0
III(1)	1.9	1.4	0.45	1.4	1.3	0.71	1.2	1.2	1.2
III(2)	1.7	1.3	0.52	1.3	1.2	0.79	1.1	1.1	1.1
III(3)	1.6	1.3	0.57	1.2	1.2	0.83	1.1	1.1	1.1

Table A2A: Ratios of the rate of proton decay that would occur if chargino diagrams contributed only versus total proton decay rate for the three most dominant decay modes, for various values of the GUT scale parameters, when the \mathcal{O}_{13} operator is included.

run no.	$\frac{\Gamma^{\text{chargino}}_{n \rightarrow K^0 \bar{\nu}}}{\Gamma^{\text{total}}_{n \rightarrow K^0 \bar{\nu}}}$			$\frac{\Gamma^{\text{chargino}}_{n \rightarrow \pi^0 \bar{\nu}}}{\Gamma^{\text{total}}_{n \rightarrow \pi^0 \bar{\nu}}}$			$\frac{\Gamma^{\text{chargino}}_{n \rightarrow \eta \bar{\nu}}}{\Gamma^{\text{total}}_{n \rightarrow \eta \bar{\nu}}}$			$\frac{\Gamma^{\text{chargino}}_{n \rightarrow \pi^- \mu^+}}{\Gamma^{\text{total}}_{n \rightarrow \pi^- \mu^+}}$		
	max	$\beta = -\alpha$	min	max	$\beta = -\alpha$	min	max	$\beta = -\alpha$	min	max	$\beta = -\alpha$	min
I	1.1	1.1	0.87	1.1	1.1	0.87	1.1	0.99	0.97	0.81	0.81	0.81
II	1.3	1.2	0.73	1.3	1.2	0.73	1.2	0.99	0.96	0.64	0.64	0.64
III(1)	1.4	1.3	0.71	1.4	1.3	0.71	2.2	0.44	0.40	0.43	0.43	0.43
III(2)	1.2	1.2	0.80	1.3	1.2	0.79	2.2	0.42	0.39	0.55	0.55	0.55
III(3)	1.2	1.1	0.84	1.2	1.2	0.83	2.2	0.43	0.41	0.63	0.63	0.63

Table A2B: Ratios of the rate of neutron decay that would occur if chargino diagrams contributed only versus total neutron decay rate, for various values of the GUT scale parameters, when the \mathcal{O}_{13} operator is included.

run no.	$\frac{\Gamma^{\text{gluino}}_{p \rightarrow K^+ \bar{\nu}}}{\Gamma^{\text{total}}_{p \rightarrow K^+ \bar{\nu}}}$			$\frac{\Gamma^{\text{gluino}}_{p \rightarrow \pi^+ \bar{\nu}}}{\Gamma^{\text{total}}_{p \rightarrow \pi^+ \bar{\nu}}}$			$\frac{\Gamma^{\text{gluino}}_{p \rightarrow K^0 \mu^+}}{\Gamma^{\text{total}}_{p \rightarrow K^0 \mu^+}}$		
	max	$\beta = -\alpha$	min	max	$\beta = -\alpha$	min	max	$\beta = -\alpha$	min
I	0.019	0.010	0.010	0.0060	0.0038	0.0038	0.00038	0.00038	0.00038
II	0.085	0.053	0.051	0.036	0.024	0.023	0.00067	0.00067	0.00067
III(1)	0.25	0.15	0.11	0.035	0.030	0.023	0.020	0.020	0.020
III(2)	0.16	0.10	0.076	0.016	0.014	0.012	0.013	0.013	0.013
III(3)	0.10	0.071	0.055	0.0099	0.0090	0.0078	0.010	0.010	0.010

Table A3A: Ratios of the rate of proton decay that would occur if gluino diagrams contributed only versus total proton decay rate for the three most dominant decay modes, for various values of the GUT scale parameters, when the \mathcal{O}_{13} operator is included.

run no.	$\frac{\Gamma^{\text{gluino}}_{n \rightarrow K^0 \bar{\nu}}}{\Gamma^{\text{total}}_{n \rightarrow K^0 \bar{\nu}}}$			$\frac{\Gamma^{\text{gluino}}_{n \rightarrow \pi^0 \bar{\nu}}}{\Gamma^{\text{total}}_{n \rightarrow \pi^0 \bar{\nu}}}$			$\frac{\Gamma^{\text{gluino}}_{n \rightarrow \eta \bar{\nu}}}{\Gamma^{\text{total}}_{n \rightarrow \eta \bar{\nu}}}$			$\frac{\Gamma^{\text{gluino}}_{n \rightarrow \pi^- \mu^+}}{\Gamma^{\text{total}}_{n \rightarrow \pi^- \mu^+}}$		
	max	$\beta = -\alpha$	min	max	$\beta = -\alpha$	min	max	$\beta = -\alpha$	min	max	$\beta = -\alpha$	min
I	0.0055	0.0034	0.0034	0.0060	0.0038	0.0038	0.025	0.025	0.019	0.0099	0.0099	0.0099
II	0.033	0.021	0.020	0.036	0.024	0.023	0.11	0.11	0.087	0.043	0.043	0.043
III(1)	0.033	0.028	0.023	0.035	0.030	0.023	0.83	0.41	0.32	0.20	0.20	0.20
III(2)	0.014	0.012	0.010	0.016	0.014	0.012	0.60	0.28	0.22	0.20	0.20	0.20
III(3)	0.0087	0.0080	0.0070	0.0099	0.0090	0.0078	0.47	0.22	0.17	0.16	0.16	0.16

Table A3B: Ratios of the rate of neutron decay that would occur if gluino diagrams contributed only versus total neutron decay rate for various values of the GUT scale parameters, when the \mathcal{O}_{13} operator is included.

run no.	$\sqrt{\frac{\Gamma_{p \rightarrow K^+ \bar{\nu}_l}^{\text{LLRR}}}{\Gamma_{p \rightarrow K^+ \bar{\nu}_l}^{\text{LLLL}}}}$			$\sqrt{\frac{\Gamma_{p \rightarrow \pi^+ \bar{\nu}_l}^{\text{LLRR}}}{\Gamma_{p \rightarrow \pi^+ \bar{\nu}_l}^{\text{LLLL}}}}$		
	$\bar{\nu}_e$	$\bar{\nu}_\mu$	$\bar{\nu}_\tau$	$\bar{\nu}_e$	$\bar{\nu}_\mu$	$\bar{\nu}_\tau$
I	0.000084	0.011	2.0	0.00019	0.024	7.3
II	0.000086	0.011	1.8	0.00020	0.025	6.4
III(1)	0.00021	0.029	3.8	0.00056	0.068	10.
III(2)	0.00026	0.040	4.6	0.00067	0.097	14.
III(3)	0.00031	0.048	5.7	0.00080	0.12	17.

Table A4: Ratios of the rate of proton decay that would occur if LLLL operators contributed only versus the rate of proton decay that would occur if LLRR operators contributed only, for each of the three anti-neutrino generations, for various values of the GUT scale parameters, when the \mathcal{O}_{13} operator is included.

run no.	$\sqrt{\frac{\Gamma_{p \rightarrow K^+ \bar{\nu}_e}^{\text{LLLL}}}{\Gamma_{p \rightarrow K^+ \bar{\nu}_e}^{\text{LLRR}}}}$	$\sqrt{\frac{\Gamma_{p \rightarrow K^+ \bar{\nu}_\mu}^{\text{LLLL}}}{\Gamma_{p \rightarrow K^+ \bar{\nu}_\mu}^{\text{LLRR}}}}$	$\sqrt{\frac{\Gamma_{p \rightarrow K^+ \bar{\nu}_\tau}^{\text{LLLL}}}{\Gamma_{p \rightarrow K^+ \bar{\nu}_\tau}^{\text{LLRR}}}}$	$\sqrt{\frac{\Gamma_{p \rightarrow K^+ \bar{\nu}_e}^{\text{LLRR}}}{\Gamma_{p \rightarrow K^+ \bar{\nu}_e}^{\text{LLLL}}}}$	$\sqrt{\frac{\Gamma_{p \rightarrow K^+ \bar{\nu}_\mu}^{\text{LLRR}}}{\Gamma_{p \rightarrow K^+ \bar{\nu}_\mu}^{\text{LLLL}}}}$	$\sqrt{\frac{\Gamma_{p \rightarrow K^+ \bar{\nu}_\tau}^{\text{LLRR}}}{\Gamma_{p \rightarrow K^+ \bar{\nu}_\tau}^{\text{LLLL}}}}$
	I	0.082	6.8×10^{-6}	1.5	0.017	0.49
II	0.10	8.6×10^{-6}	1.9	0.021	0.56	
III(1)	0.035	7.2×10^{-6}	0.60	0.017	0.26	
III(2)	0.032	8.2×10^{-6}	0.49	0.020	0.22	
III(3)	0.026	8.1×10^{-6}	0.41	0.020	0.18	

Table A5A: Ratios of partial decay rates for $p \rightarrow K^+ \bar{\nu}$, which compare the importance of the LLLL and LLRR operators for each generation of anti-neutrino versus contribution of the LLRR operator of the third generation anti-neutrino for various values of the GUT scale parameters, when the \mathcal{O}_{13} operator is included.

run no.	$\sqrt{\frac{\Gamma_{p \rightarrow \pi^+ \bar{\nu}_e}^{\text{LLLL}}}{\Gamma_{p \rightarrow \pi^+ \bar{\nu}_e}^{\text{LLRR}}}}$	$\sqrt{\frac{\Gamma_{p \rightarrow \pi^+ \bar{\nu}_\mu}^{\text{LLLL}}}{\Gamma_{p \rightarrow \pi^+ \bar{\nu}_\mu}^{\text{LLRR}}}}$	$\sqrt{\frac{\Gamma_{p \rightarrow \pi^+ \bar{\nu}_\tau}^{\text{LLLL}}}{\Gamma_{p \rightarrow \pi^+ \bar{\nu}_\tau}^{\text{LLRR}}}}$	$\sqrt{\frac{\Gamma_{p \rightarrow \pi^+ \bar{\nu}_e}^{\text{LLRR}}}{\Gamma_{p \rightarrow \pi^+ \bar{\nu}_e}^{\text{LLLL}}}}$	$\sqrt{\frac{\Gamma_{p \rightarrow \pi^+ \bar{\nu}_\mu}^{\text{LLRR}}}{\Gamma_{p \rightarrow \pi^+ \bar{\nu}_\mu}^{\text{LLLL}}}}$	$\sqrt{\frac{\Gamma_{p \rightarrow \pi^+ \bar{\nu}_\tau}^{\text{LLRR}}}{\Gamma_{p \rightarrow \pi^+ \bar{\nu}_\tau}^{\text{LLLL}}}}$
	I	0.026	4.8×10^{-6}	0.48	0.012	0.14
II	0.030	6.1×10^{-6}	0.59	0.015	0.16	
III(1)	0.0095	5.3×10^{-6}	0.18	0.013	0.098	
III(2)	0.0081	5.4×10^{-6}	0.13	0.013	0.071	
III(3)	0.0067	5.4×10^{-6}	0.11	0.013	0.058	

Table A5B: Ratios of partial decay rates for $p \rightarrow \pi^+ \bar{\nu}$, which compare the importance of the LLLL and LLRR operators for each generation of anti-neutrino versus contribution of the LLRR operator of the third generation anti-neutrino for various values of the GUT scale parameters, when the \mathcal{O}_{13} operator is included.

run no.	I	II	III(1)	III(2)	III(3)
$\tilde{\alpha}_{GUT}^{-1}$	24.43	24.36	24.51	24.65	24.75
M_{GUT}	2.498×10^{16}	3.172×10^{16}	3.327×10^{16}	2.857×10^{16}	2.513×10^{16}
ϵ_3	-0.04760	-0.04886	-0.04342	-0.04420	-0.04550
A	0.7640	0.8067	0.8523	0.8867	0.8872
B	0.05259	0.05439	0.05630	0.05882	0.05956
C	0.0001096	0.0001155	0.0001213	0.0001231	0.0001226
E	0.01251	0.01308	0.01360	0.01397	0.01397
ϕ	1.066	1.041	1.020	1.023	1.038
D	0.0004633	0.0004944	0.0005064	0.0005691	0.0005665
δ	5.698	5.706	5.698	5.742	5.744
$\tan \beta$	52.77	54.38	55.39	55.86	55.92
$\mu(M_Z)$	80.0	80.0	160.	240.	300.
$m_{1/2}$	280.	240.	170.	170.	170.
m_0	400.	700.	1400.	1400.	1400.
m_{H_d}	706.4	994.6	1858.	1859.	1855.
m_{H_u}	635.6	865.3	1599.	1591.	1585.
A_0	322.2	458.4	-982.4	-1079.	-1274.

Table A6: Values of the GUT scale parameters used in Tables A1 through A5. All dimensions in GeV units.

run no.	model	$\frac{\tau(p \rightarrow K^+ \bar{\nu})}{10^{32} \text{ yrs}}$	$\frac{\Gamma(p \rightarrow \pi^+ \bar{\nu})}{\Gamma(p \rightarrow K^+ \bar{\nu})}$	$\frac{\Gamma(p \rightarrow K^0 \mu^+)}{\Gamma(p \rightarrow K^+ \bar{\nu})}$	$\frac{\Gamma(p \rightarrow \pi^0 \mu^+)}{\Gamma(p \rightarrow K^+ \bar{\nu})}$	$\frac{\Gamma(p \rightarrow \eta \mu^+)}{\Gamma(p \rightarrow K^+ \bar{\nu})}$
I	<i>a</i>	7.3	0.22	0.0020	0.0011	0.00039
	<i>b</i>	3.5	0.17	0.0032	0.0017	0.00060
	<i>c</i>	11.	0.25	0.0012	0.00067	0.00024
	<i>d</i>	4.1	0.15	0.0047	0.0023	0.00082
	<i>e</i>	14.	0.25	0.0028	0.0013	0.00045
	<i>f</i>	2.0	0.13	0.0049	0.0024	0.00086
II	<i>a</i>	23.	0.21	0.0028	0.0015	0.00054
	<i>b</i>	10.	0.16	0.0040	0.0021	0.00076
	<i>c</i>	36.	0.24	0.0018	0.00098	0.00034
	<i>d</i>	10.	0.15	0.0050	0.0025	0.00087
	<i>e</i>	39.	0.23	0.0036	0.0016	0.00055
	<i>f</i>	4.9	0.13	0.0051	0.0026	0.00090
III(1)	<i>a</i>	59.	0.30	0.00078	0.00034	0.00011
	<i>b</i>	68.	0.28	0.0023	0.0012	0.00039
	<i>c</i>	68.	0.31	0.00052	0.00017	0.000044
	<i>d</i>	32.	0.24	0.0016	0.00072	0.00025
	<i>e</i>	57.	0.30	0.00080	0.00025	0.000076
	<i>f</i>	21.	0.21	0.0021	0.00097	0.00034
III(2)	<i>a</i>	26.	0.31	0.00048	0.00017	0.000048
	<i>b</i>	33.	0.32	0.0013	0.00059	0.00019
	<i>c</i>	29.	0.32	0.00039	0.000094	0.000019
	<i>d</i>	18.	0.27	0.0010	0.00042	0.00014
	<i>e</i>	26.	0.32	0.00053	0.00014	0.000036
	<i>f</i>	13.	0.24	0.0014	0.00062	0.00021
III(3)	<i>a</i>	18.	0.31	0.00040	0.00012	0.000031
	<i>b</i>	23.	0.34	0.0010	0.00040	0.00012
	<i>c</i>	20.	0.32	0.00034	0.000073	0.000012
	<i>d</i>	14.	0.28	0.00081	0.00031	0.000099
	<i>e</i>	19.	0.32	0.00044	0.00010	0.000024
	<i>f</i>	11.	0.26	0.0011	0.00047	0.00016

Table B1A: Partial mean lifetime for proton decaying into kaon plus anti-neutrino and ratios of the rates of proton decay into various decay products versus rate of decay into kaon plus anti-neutrino for various values of the GUT scale parameters, when the \mathcal{O}_{13} operator is not included. For all entries, $\beta = -\alpha$.

run no.	model	$\frac{\tau(n \rightarrow K^0 \bar{\nu})}{10^{32} \text{ yrs}}$	$\frac{\Gamma(n \rightarrow \pi^0 \bar{\nu})}{\Gamma(n \rightarrow K^0 \bar{\nu})}$	$\frac{\Gamma(n \rightarrow \eta \bar{\nu})}{\Gamma(n \rightarrow K^0 \bar{\nu})}$	$\frac{\Gamma(n \rightarrow \pi^- \mu^+)}{\Gamma(n \rightarrow K^0 \bar{\nu})}$
I	<i>a</i>	2.4	0.036	0.0020	0.00071
	<i>b</i>	1.4	0.033	0.0047	0.0013
	<i>c</i>	3.1	0.036	0.00095	0.00038
	<i>d</i>	1.9	0.035	0.010	0.0022
	<i>e</i>	4.0	0.036	0.0039	0.00073
	<i>f</i>	1.0	0.035	0.012	0.0025
II	<i>a</i>	8.0	0.035	0.0028	0.0011
	<i>b</i>	4.2	0.033	0.0063	0.0018
	<i>c</i>	11.	0.036	0.0015	0.00059
	<i>d</i>	4.8	0.035	0.010	0.0024
	<i>e</i>	12.	0.036	0.0044	0.0010
	<i>f</i>	2.5	0.034	0.011	0.0026
III(1)	<i>a</i>	16.	0.039	0.0011	0.00018
	<i>b</i>	17.	0.036	0.0038	0.00060
	<i>c</i>	17.	0.038	0.00075	0.000082
	<i>d</i>	9.9	0.037	0.0015	0.00044
	<i>e</i>	14.	0.036	0.00037	0.00012
	<i>f</i>	7.4	0.036	0.0026	0.00068
III(2)	<i>a</i>	6.6	0.039	0.00066	0.000086
	<i>b</i>	7.4	0.037	0.0020	0.00027
	<i>c</i>	7.0	0.038	0.00051	0.000045
	<i>d</i>	5.0	0.037	0.00085	0.00023
	<i>e</i>	6.1	0.036	0.00028	0.000064
	<i>f</i>	4.1	0.037	0.0015	0.00038
III(3)	<i>a</i>	4.5	0.039	0.00054	0.000060
	<i>b</i>	5.1	0.037	0.0014	0.00018
	<i>c</i>	4.8	0.038	0.00044	0.000034
	<i>d</i>	3.7	0.037	0.00064	0.00017
	<i>e</i>	4.3	0.037	0.00026	0.000047
	<i>f</i>	3.2	0.038	0.0011	0.00028

Table B1B: Partial mean lifetime for neutron decaying into kaon plus anti-neutrino and ratios of the rates of neutron decay into various decay products versus rate of decay into kaon plus anti-neutrino for various values of the GUT scale parameters, when the \mathcal{O}_{13} operator is not included. For all entries, $\beta = -\alpha$.

run no.	model	$\frac{\Gamma_{p \rightarrow K^+ \bar{\nu}}^{\text{chargino}}}{\Gamma_{p \rightarrow K^+ \bar{\nu}}^{\text{total}}}$			$\frac{\Gamma_{p \rightarrow \pi^+ \bar{\nu}}^{\text{chargino}}}{\Gamma_{p \rightarrow \pi^+ \bar{\nu}}^{\text{total}}}$			$\frac{\Gamma_{p \rightarrow K^0 \mu^+}^{\text{chargino}}}{\Gamma_{p \rightarrow K^0 \mu^+}^{\text{total}}}$		
		max	$\beta = -\alpha$	min	max	$\beta = -\alpha$	min	max	$\beta = -\alpha$	min
I	a	1.2	1.1	0.85	1.1	1.1	0.87	1.0	1.0	1.0
	b	1.2	1.2	0.93	1.2	1.2	0.86	1.0	1.0	1.0
	c	1.2	1.1	0.83	1.1	1.1	0.89	0.99	0.99	0.99
	d	1.2	0.99	0.98	1.2	0.92	0.91	1.0	1.0	1.0
	e	1.2	0.91	0.91	1.1	0.91	0.91	1.0	1.0	1.0
	f	1.2	1.0	1.0	1.2	0.97	0.94	1.0	1.0	1.0
II	a	1.5	1.3	0.72	1.4	1.3	0.72	1.0	1.0	1.0
	b	1.4	1.4	0.90	1.4	1.4	0.75	1.0	1.0	1.0
	c	1.4	1.3	0.65	1.3	1.2	0.75	1.0	1.0	1.0
	d	1.4	1.0	1.0	1.4	0.88	0.86	1.0	1.0	1.0
	e	1.4	0.84	0.84	1.3	0.81	0.81	1.0	1.0	1.0
	f	1.4	1.1	1.1	1.4	0.97	0.93	1.0	1.0	1.0
III(1)	a	1.9	1.5	0.53	1.5	1.3	0.69	1.1	1.1	1.1
	b	2.6	2.4	0.34	2.0	2.0	0.47	1.2	1.2	1.2
	c	1.6	1.4	0.62	1.3	1.2	0.76	1.2	1.2	1.2
	d	2.7	0.48	0.42	2.0	0.53	0.50	1.1	1.1	1.1
	e	1.7	0.65	0.65	1.3	0.76	0.76	0.98	0.98	0.98
	f	2.8	0.53	0.42	2.3	0.50	0.42	1.1	1.1	1.1
III(2)	a	1.5	1.3	0.65	1.3	1.2	0.78	1.1	1.1	1.1
	b	2.2	2.0	0.42	1.6	1.6	0.59	1.2	1.2	1.2
	c	1.4	1.2	0.72	1.2	1.2	0.83	1.1	1.1	1.1
	d	2.2	0.52	0.47	1.6	0.62	0.60	1.0	1.0	1.0
	e	1.4	0.74	0.74	1.2	0.83	0.83	0.99	0.99	0.99
	f	2.5	0.51	0.41	1.9	0.56	0.50	1.1	1.1	1.1
III(3)	a	1.4	1.3	0.70	1.2	1.2	0.81	1.1	1.1	1.1
	b	1.9	1.8	0.48	1.5	1.5	0.65	1.1	1.1	1.1
	c	1.3	1.2	0.77	1.2	1.1	0.86	1.1	1.1	1.1
	d	1.9	0.56	0.52	1.5	0.67	0.66	1.0	1.0	1.0
	e	1.3	0.78	0.78	1.2	0.86	0.86	0.99	0.99	0.99
	f	2.3	0.53	0.44	1.7	0.61	0.56	1.1	1.1	1.1

Table B2A: Ratios of the rate of proton decay that would occur if chargino diagrams contributed only versus total proton decay rate for the three most dominant decay modes, for various values of the GUT scale parameters, when the \mathcal{O}_{13} operator is not included.

run no.	model	$\frac{\Gamma_{n \rightarrow K^0 \bar{\nu}}^{\text{chargino}}}{\Gamma_{n \rightarrow K^0 \bar{\nu}}^{\text{total}}}$			$\frac{\Gamma_{n \rightarrow \pi^0 \bar{\nu}}^{\text{chargino}}}{\Gamma_{n \rightarrow \pi^0 \bar{\nu}}^{\text{total}}}$			$\frac{\Gamma_{n \rightarrow \eta \bar{\nu}}^{\text{chargino}}}{\Gamma_{n \rightarrow \eta \bar{\nu}}^{\text{total}}}$		
		max	$\beta = -\alpha$	min	max	$\beta = -\alpha$	min	max	$\beta = -\alpha$	min
I	<i>a</i>	1.2	1.1	0.85	1.1	1.1	0.87	1.2	1.1	1.0
	<i>b</i>	1.2	1.2	0.86	1.2	1.2	0.86	1.1	1.1	1.1
	<i>c</i>	1.1	1.1	0.87	1.1	1.1	0.89	1.2	0.95	0.92
	<i>d</i>	1.2	0.92	0.92	1.2	0.92	0.91	1.1	1.1	1.1
	<i>e</i>	1.1	0.91	0.91	1.1	0.91	0.91	1.2	1.2	1.1
	<i>f</i>	1.2	0.98	0.96	1.2	0.97	0.94	1.1	1.1	1.1
II	<i>a</i>	1.4	1.3	0.70	1.4	1.3	0.72	1.4	1.1	1.1
	<i>b</i>	1.4	1.4	0.76	1.4	1.4	0.75	1.3	1.1	1.1
	<i>c</i>	1.3	1.3	0.71	1.3	1.2	0.75	1.4	0.92	0.88
	<i>d</i>	1.4	0.89	0.88	1.4	0.88	0.86	1.3	1.3	1.2
	<i>e</i>	1.3	0.81	0.81	1.3	0.81	0.81	1.4	1.4	1.2
	<i>f</i>	1.4	0.99	0.97	1.4	0.97	0.93	1.3	1.3	1.2
III(1)	<i>a</i>	1.6	1.4	0.64	1.5	1.3	0.69	3.1	0.53	0.43
	<i>b</i>	2.1	2.1	0.43	2.0	2.0	0.47	1.9	0.64	0.63
	<i>c</i>	1.4	1.3	0.72	1.3	1.2	0.76	3.1	0.35	0.31
	<i>d</i>	2.2	0.49	0.47	2.0	0.53	0.50	2.1	2.1	0.87
	<i>e</i>	1.4	0.75	0.75	1.3	0.76	0.76	3.1	2.9	0.65
	<i>f</i>	2.5	0.46	0.41	2.3	0.50	0.42	1.8	1.8	0.94
III(2)	<i>a</i>	1.3	1.3	0.74	1.3	1.2	0.78	3.1	0.48	0.38
	<i>b</i>	1.7	1.7	0.55	1.6	1.6	0.59	2.2	0.52	0.51
	<i>c</i>	1.2	1.2	0.81	1.2	1.2	0.83	2.8	0.40	0.36
	<i>d</i>	1.7	0.58	0.57	1.6	0.62	0.60	2.4	2.4	0.72
	<i>e</i>	1.2	0.83	0.82	1.2	0.83	0.83	2.7	2.6	0.55
	<i>f</i>	2.1	0.52	0.47	1.9	0.56	0.50	2.1	2.0	0.82
III(3)	<i>a</i>	1.3	1.2	0.78	1.2	1.2	0.81	2.9	0.49	0.39
	<i>b</i>	1.6	1.6	0.61	1.5	1.5	0.65	2.4	0.47	0.46
	<i>c</i>	1.2	1.2	0.84	1.2	1.1	0.86	2.4	0.45	0.41
	<i>d</i>	1.6	0.64	0.63	1.5	0.67	0.66	2.5	2.5	0.64
	<i>e</i>	1.2	0.86	0.85	1.2	0.86	0.86	2.4	2.3	0.54
	<i>f</i>	1.9	0.57	0.53	1.7	0.61	0.56	2.2	2.1	0.75

Table B2B: Ratios of the rate of neutron decay that would occur if chargino diagrams contributed only versus total neutron decay rate for various values of the GUT scale parameters, when the \mathcal{O}_{13} operator is not included.

run no.	m o d e l	$\sqrt{\frac{\Gamma_{LLRR}^{p \rightarrow K^+ \bar{\nu}_l}}{\Gamma_{LLLL}^{p \rightarrow K^+ \bar{\nu}_l}}}$			$\sqrt{\frac{\Gamma_{LLRR}^{p \rightarrow \pi^+ \bar{\nu}_l}}{\Gamma_{LLLL}^{p \rightarrow \pi^+ \bar{\nu}_l}}}$		
		$\bar{\nu}_e$	$\bar{\nu}_\mu$	$\bar{\nu}_\tau$	$\bar{\nu}_e$	$\bar{\nu}_\mu$	$\bar{\nu}_\tau$
I	a	0.000044	0.011	4.2	0.000073	0.018	8.4
	b	0.000022	0.0049	1.9	0.000037	0.0083	3.6
	c	0.000065	0.017	5.7	0.00011	0.029	12.
	d	0.000022	0.0043	1.7	0.000037	0.0071	2.8
	e	0.000062	0.011	4.2	0.00010	0.018	6.5
	f	0.000015	0.0031	1.3	0.000025	0.0050	2.1
II	a	0.000048	0.011	5.1	0.000078	0.018	10.
	b	0.000023	0.0049	2.6	0.000038	0.0083	5.4
	c	0.000071	0.017	5.7	0.00012	0.029	11.
	d	0.000022	0.0044	2.2	0.000037	0.0073	3.5
	e	0.000061	0.011	4.2	0.00010	0.019	6.4
	f	0.000015	0.0031	1.7	0.000025	0.0051	2.7
III(1)	a	0.00019	0.032	6.4	0.00031	0.055	10.
	b	0.000071	0.013	3.4	0.00012	0.023	5.8
	c	0.00030	0.045	7.6	0.00049	0.079	12.
	d	0.000059	0.014	3.8	0.000098	0.022	6.8
	e	0.00015	0.042	8.5	0.00025	0.064	16.
	f	0.000042	0.0093	2.8	0.000069	0.015	4.8
III(2)	a	0.00029	0.048	10.	0.00046	0.081	16.
	b	0.00011	0.020	5.3	0.00018	0.034	9.1
	c	0.00044	0.066	12.	0.00072	0.12	19.
	d	0.000088	0.020	6.1	0.00014	0.032	11.
	e	0.00023	0.061	13.	0.00037	0.095	24.
	f	0.000062	0.014	4.4	0.00010	0.022	7.6
III(3)	a	0.00035	0.058	13.	0.00056	0.099	20.
	b	0.00013	0.024	6.8	0.00022	0.042	12.
	c	0.00054	0.081	15.	0.00088	0.14	24.
	d	0.00011	0.024	7.8	0.00018	0.040	14.
	e	0.00028	0.075	16.	0.00046	0.12	30.
	f	0.000076	0.017	5.6	0.00012	0.027	9.7

Table B4: Ratios of the rate of proton decay that would occur if LLLL operators contributed only versus the rate of proton decay that would occur if LLRR operators contributed only, for each of the three anti-neutrino generations, for various values of the GUT scale parameters, when the \mathcal{O}_{13} operator is not included.

run no.	model	$\frac{\Gamma_{p \rightarrow K^+ \bar{\nu}_e}}{\Gamma_{p \rightarrow K^+ \bar{\nu}_\tau}}$	$\frac{\Gamma_{p \rightarrow K^+ \bar{\nu}_\mu}}{\Gamma_{p \rightarrow K^+ \bar{\nu}_\tau}}$	$\frac{\Gamma_{p \rightarrow K^+ \bar{\nu}_\mu}}{\Gamma_{p \rightarrow K^+ \bar{\nu}_\tau}}$	$\frac{\Gamma_{p \rightarrow K^+ \bar{\nu}_\mu}}{\Gamma_{p \rightarrow K^+ \bar{\nu}_\tau}}$	$\frac{\Gamma_{p \rightarrow K^+ \bar{\nu}_\tau}}{\Gamma_{p \rightarrow K^+ \bar{\nu}_\tau}}$
		LLLL	LLRR	LLLL	LLRR	LLLL
I	<i>a</i>	0.062	2.8×10^{-6}	0.78	0.0084	0.24
	<i>b</i>	0.13	2.8×10^{-6}	1.7	0.0085	0.53
	<i>c</i>	0.043	2.8×10^{-6}	0.49	0.0085	0.18
	<i>d</i>	0.12	2.8×10^{-6}	1.9	0.0084	0.57
	<i>e</i>	0.045	2.8×10^{-6}	0.80	0.0085	0.24
	<i>f</i>	0.17	2.7×10^{-6}	2.7	0.0082	0.79
II	<i>a</i>	0.071	3.4×10^{-6}	0.95	0.010	0.20
	<i>b</i>	0.15	3.5×10^{-6}	2.1	0.011	0.38
	<i>c</i>	0.049	3.5×10^{-6}	0.61	0.010	0.18
	<i>d</i>	0.15	3.4×10^{-6}	2.3	0.010	0.45
	<i>e</i>	0.057	3.5×10^{-6}	0.94	0.011	0.24
	<i>f</i>	0.22	3.3×10^{-6}	3.2	0.010	0.60
III(1)	<i>a</i>	0.015	3.0×10^{-6}	0.28	0.0091	0.16
	<i>b</i>	0.043	3.0×10^{-6}	0.69	0.0092	0.30
	<i>c</i>	0.010	3.0×10^{-6}	0.21	0.0092	0.13
	<i>d</i>	0.050	3.0×10^{-6}	0.67	0.0091	0.26
	<i>e</i>	0.020	3.0×10^{-6}	0.22	0.0092	0.12
	<i>f</i>	0.069	2.9×10^{-6}	0.95	0.0089	0.36
III(2)	<i>a</i>	0.010	3.0×10^{-6}	0.19	0.0090	0.10
	<i>b</i>	0.029	3.0×10^{-6}	0.46	0.0091	0.19
	<i>c</i>	0.0068	3.0×10^{-6}	0.14	0.0091	0.085
	<i>d</i>	0.034	3.0×10^{-6}	0.45	0.0090	0.16
	<i>e</i>	0.013	3.0×10^{-6}	0.15	0.0091	0.076
	<i>f</i>	0.047	2.9×10^{-6}	0.64	0.0088	0.23
III(3)	<i>a</i>	0.0086	3.0×10^{-6}	0.16	0.0091	0.080
	<i>b</i>	0.023	3.0×10^{-6}	0.38	0.0092	0.15
	<i>c</i>	0.0056	3.0×10^{-6}	0.11	0.0091	0.068
	<i>d</i>	0.028	3.0×10^{-6}	0.37	0.0090	0.13
	<i>e</i>	0.011	3.0×10^{-6}	0.12	0.0092	0.061
	<i>f</i>	0.038	2.9×10^{-6}	0.53	0.0089	0.18

Table B5A: Ratios of partial decay rates for $p \rightarrow K^+ \bar{\nu}$, which compare the importance of the LLLL and LLRR operators for each generation of anti-neutrino versus contribution of the LLRR operator of the third generation anti-neutrino for various values of the GUT scale parameters, when the \mathcal{O}_{13} operator is not included.

run no.	model	$\frac{\text{LLLL}}{\text{LLRR}}$	$\frac{\text{LLRR}}{\text{LLRR}}$	$\frac{\text{LLLL}}{\text{LLRR}}$	$\frac{\text{LLRR}}{\text{LLRR}}$	$\frac{\text{LLLL}}{\text{LLRR}}$
		$\frac{\Gamma_{p \rightarrow \pi^+ \bar{\nu}_e}}{\Gamma_{p \rightarrow \pi^+ \bar{\nu}_\tau}}$	$\frac{\Gamma_{p \rightarrow \pi^+ \bar{\nu}_e}}{\Gamma_{p \rightarrow \pi^+ \bar{\nu}_\tau}}$	$\frac{\Gamma_{p \rightarrow \pi^+ \bar{\nu}_\mu}}{\Gamma_{p \rightarrow \pi^+ \bar{\nu}_\tau}}$	$\frac{\Gamma_{p \rightarrow \pi^+ \bar{\nu}_\mu}}{\Gamma_{p \rightarrow \pi^+ \bar{\nu}_\tau}}$	$\frac{\Gamma_{p \rightarrow \pi^+ \bar{\nu}_\tau}}{\Gamma_{p \rightarrow \pi^+ \bar{\nu}_\tau}}$
I	<i>a</i>	0.038	2.8×10^{-6}	0.48	0.0085	0.12
	<i>b</i>	0.076	2.8×10^{-6}	1.0	0.0085	0.28
	<i>c</i>	0.026	2.8×10^{-6}	0.30	0.0085	0.084
	<i>d</i>	0.076	2.8×10^{-6}	1.2	0.0085	0.35
	<i>e</i>	0.027	2.8×10^{-6}	0.48	0.0085	0.15
	<i>f</i>	0.11	2.7×10^{-6}	1.7	0.0083	0.48
II	<i>a</i>	0.044	3.5×10^{-6}	0.58	0.010	0.095
	<i>b</i>	0.092	3.5×10^{-6}	1.3	0.011	0.19
	<i>c</i>	0.030	3.5×10^{-6}	0.37	0.011	0.088
	<i>d</i>	0.095	3.5×10^{-6}	1.4	0.010	0.29
	<i>e</i>	0.034	3.5×10^{-6}	0.57	0.011	0.16
	<i>f</i>	0.13	3.4×10^{-6}	2.0	0.010	0.38
III(1)	<i>a</i>	0.0097	3.0×10^{-6}	0.17	0.0092	0.096
	<i>b</i>	0.025	3.0×10^{-6}	0.40	0.0092	0.17
	<i>c</i>	0.0063	3.0×10^{-6}	0.12	0.0092	0.080
	<i>d</i>	0.031	3.0×10^{-6}	0.42	0.0092	0.15
	<i>e</i>	0.012	3.1×10^{-6}	0.14	0.0093	0.064
	<i>f</i>	0.043	3.0×10^{-6}	0.60	0.0090	0.21
III(2)	<i>a</i>	0.0065	3.0×10^{-6}	0.11	0.0091	0.062
	<i>b</i>	0.017	3.0×10^{-6}	0.27	0.0091	0.11
	<i>c</i>	0.0042	3.0×10^{-6}	0.078	0.0091	0.052
	<i>d</i>	0.021	3.0×10^{-6}	0.28	0.0091	0.093
	<i>e</i>	0.0081	3.0×10^{-6}	0.096	0.0092	0.042
	<i>f</i>	0.029	2.9×10^{-6}	0.40	0.0089	0.13
III(3)	<i>a</i>	0.0054	3.0×10^{-6}	0.092	0.0091	0.049
	<i>b</i>	0.014	3.0×10^{-6}	0.22	0.0092	0.085
	<i>c</i>	0.0034	3.0×10^{-6}	0.064	0.0092	0.042
	<i>d</i>	0.017	3.0×10^{-6}	0.23	0.0091	0.072
	<i>e</i>	0.0066	3.0×10^{-6}	0.079	0.0092	0.034
	<i>f</i>	0.024	3.0×10^{-6}	0.33	0.0090	0.10

Table B5B: Ratios of partial decay rates for $p \rightarrow \pi^+ \bar{\nu}$, which compare the importance of the LLLL and LLRR operators for each generation of anti-neutrino versus contribution of the LLRR operator of the third generation anti-neutrino for various values of the GUT scale parameters, when the \mathcal{O}_{13} operator is not included.

run no.	I	II	III(1)	III(2)	III(3)
$\tilde{\alpha}_{GUT}^{-1}$	24.43	24.36	24.51	24.65	24.75
M_{GUT}	2.498×10^{16}	3.172×10^{16}	3.327×10^{16}	2.857×10^{16}	2.513×10^{16}
ϵ_3	-0.04760	-0.04886	-0.04342	-0.04420	-0.04550
A	0.7640	0.8067	0.8523	0.8867	0.8872
B	0.05798	0.06019	0.06254	0.06533	0.06607
C	0.00008824	0.00009204	0.00009550	0.00009801	0.00009809
E	0.01063	0.01111	0.01154	0.01182	0.01180
ϕ	1.762	1.765	1.767	1.765	1.763
$\tan \beta$	52.71	54.31	55.32	55.79	55.87
$\mu(M_Z)$	80.0	80.0	160.	240.	300.
$m_{1/2}$	280.	240.	170.	170.	170.
m_0	400.	700.	1400.	1400.	1400.
m_{H_d}	706.3	994.4	1858.	1859.	1855.
m_{H_u}	635.9	865.6	1599.	1592.	1585.
A_0	322.2	458.4	-982.4	-1079.	-1274.

Table B6: Values of the GUT scale parameters used in Tables B1 through B5. All dimensions in GeV units.

5 Discussion of the results

5.1 Overall Rates

Many significant results appear from the tables of the previous section. First, comparing the rates of proton decay predicted in the tables above with the results of experimental searches for proton and baryon-number violating neutron decay summarized in Table 4, it can be seen that the predicted upper bounds on the lifetimes for nucleon decay are above, and, in most cases, well above, the experimental lower bounds. The loop integral $I(M_{gaugino}, M_{(slepton)}^{squark}, M_{(slepton)}^{squark})$ goes roughly like $1/M_{(slepton)}^{2squark}$ in the limit where squarks and sleptons are much heavier than gauginos. Hence, the decay rates go naively like $(m_{1/2}^2 + \mu_R^2)/m_0^4$, where $\mu_R \equiv \mu(M_Z)$. This approximation roughly explains the dependence of the nucleon decay rates on m_0 , $\mu(M_Z)$, and $m_{1/2}$ seen in Tables A1A, A1B, B1A, and B1B.

5.2 LLRR vs. LLLL Operators

Secondly, LLRR operators dominate over LLLL operators for the third generation anti-neutrino, for the decays into $K\bar{\nu}$ and $\pi\bar{\nu}$. (See Tables A4 and B4.) We

Table 4: Current experimental lower bounds on the various partial lifetimes of the nucleons [19]

$\tau(p \rightarrow K^+\bar{\nu})$	$>$	1.0×10^{32} yrs
$\tau(p \rightarrow \pi^+\bar{\nu})$	$>$	$.25 \times 10^{32}$ yrs
$\tau(p \rightarrow \pi^0\mu^+)$	$>$	2.7×10^{32} yrs
$\tau(p \rightarrow \eta\mu^+)$	$>$	$.69 \times 10^{32}$ yrs
$\tau(p \rightarrow \pi^0e^+)$	$>$	5.5×10^{32} yrs
$\tau(p \rightarrow \eta e^+)$	$>$	1.4×10^{32} yrs
$\tau(n \rightarrow K^0\bar{\nu})$	$>$	$.86 \times 10^{32}$ yrs
$\tau(n \rightarrow \pi^0\bar{\nu})$	$>$	1.0×10^{32} yrs
$\tau(n \rightarrow \eta\bar{\nu})$	$>$	$.54 \times 10^{32}$ yrs
$\tau(n \rightarrow \pi^-\mu^+)$	$>$	1.0×10^{32} yrs
$\tau(n \rightarrow \pi^-e^+)$	$>$	1.3×10^{32} yrs

can gain an intuitive understanding of why this is if we neglect the gluino contribution to the decay rates and look at approximate formulas for the rate of decay due to charginos. The loop integral $I(a, b, c)$ is a relatively smooth function of the masses and as a result, to a very good approximation, when calculating chargino diagrams for the third generation anti-neutrino, sums over gamma matrices of the form $\Gamma_{L\lambda i}\Gamma_{R\lambda j}^*I(\tilde{\Omega}_\lambda, b, c)$ are approximately zero while sums of the form $\Gamma_{L\lambda i}\Gamma_{L\lambda j}^*I(\tilde{\Omega}_\lambda, b, c)$ and $\Gamma_{R\lambda i}\Gamma_{R\lambda j}^*I(\tilde{\Omega}_\lambda, b, c)$ are approximately equal to $\delta_{ij}I(\tilde{\Omega}_{i_L}, b, c)$ and $\delta_{ij}I(\tilde{\Omega}_{i_R}, b, c)$, respectively, due to the orthogonality of the gamma matrices. Hence,

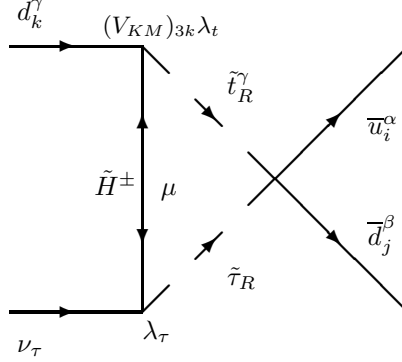
$$\begin{aligned}
C_{1jk3}^{(\overline{ud})(d\nu)} &\approx \\
\frac{1}{16\pi^2 M_t} (\Gamma_{U,R} \hat{Y}_U V_{KM})_{\lambda k} \Gamma_{U,R}^* \lambda k' (\Gamma_{E,R} \hat{Y}_e)_{\rho 3} \Gamma_{E,R\rho l'}^* \hat{c}_{ud}^{[1j\hat{c}_{ue}^* k']l'} U_+ 2n U_- 2n m_{\tilde{\chi}_n} I(\tilde{\chi}_n, \tilde{u}_\lambda, \tilde{e}_\rho) \\
&\approx \frac{1}{16\pi^2 M_t} \lambda_\tau \lambda_{u_{k'}} (V_{KM})_{k'k} \hat{c}_{ud}^{[1j\hat{c}_{ue}^* k']3} U_+ 2n U_- 2n m_{\tilde{\chi}_n} I(\tilde{\chi}_n, \tilde{u}_{k'_R}, \tilde{e}_{3R}) \\
&\approx \frac{1}{16\pi^2 M_t} \lambda_\tau \lambda_t (V_{KM})_{3k} \hat{c}_{ud}^{[1j\hat{c}_{ue}^* 3]3} U_+ 2n U_- 2n m_{\tilde{\chi}_n} I(\tilde{\chi}_n, \tilde{u}_{3R}, \tilde{e}_{3R})
\end{aligned} \tag{3}$$

See fig. 2 for the Feynman diagram giving the dominant contribution to eqn. (3).

$$\begin{aligned}
C_{1jk3}^{(ud)(d\nu)} &\approx \\
\frac{1}{16\pi^2 \tilde{M}_t} U_+ 1n U_- 1n m_{\tilde{\chi}_n} \{g_2^2 (V_{KM})_{i'j} (V_{KM}^\dagger)_{j'1} \hat{c}_{qq}^{i'[j'\hat{c}_{ql}^{k}]3} I(\tilde{\chi}_n, \tilde{u}_{i'_L}, \tilde{d}_{j'_L}) \\
+ g_2^2 (V_{KM})_{k'k} \hat{c}_{qq}^{[1j\hat{c}_{ql}^{k'}]3} I(\tilde{\chi}_n, \tilde{u}_{k'_L}, \tilde{e}_{3L})\}
\end{aligned} \tag{4}$$

The loop integral factors $\sum_n U_+ a_n U_- a'n m_{\tilde{\chi}_n} I(\tilde{\chi}_n, b, c)$ can further be ap-

Figure 2: Feynman diagram that gives the dominant contribution to $C_{1jk3}^{(\overline{ud})(d\nu)}$.



proximated

$$\sum_n U_{+an} U_{-a'n} m_{\tilde{\chi}_n} I(\tilde{\chi}_n, b, c) \approx \begin{cases} M_{wino} I(\tilde{W}_\pm, b, c) & \text{if } a = a' = 1 \\ \mu_R I(\tilde{H}_\pm, b, c) & \text{if } a = a' = 2 \end{cases}.$$

Hence,

$$\frac{C_{1jk3}^{(\overline{ud})(d\nu)}}{C_{1jk3}^{(ud)(d\nu)}} \approx \frac{\mu_R}{M_{wino}} \frac{\lambda_\tau \lambda_t (V_{KM})_{3k} \hat{c}_{ud}^* [1j \hat{c}_{ue}^* 3]^3 I(\tilde{H}_\pm, \tilde{u}_{3R}, \tilde{e}_{3R})}{g_2^2 (V_{KM})_{i'j} (V_{KM}^\dagger)_{j'1} \hat{c}_{qq}^{i'j'} \hat{c}_{ql}^{k]3} I(\tilde{W}_\pm, \tilde{u}_{i_L}, \tilde{d}_{j'_L}) + g_2^2 (V_{KM})_{k'k} \hat{c}_{qq} [1j \hat{c}_{ql}^{k'}]^3 I(\tilde{W}_\pm, \tilde{u}_{k'_L}, \tilde{e}_{3_L})} \quad (5)$$

The integral $I(a, b, c)$ is approximately $\log(b^2/c^2)/(b^2 - c^2)$ in the limit where $a \ll b, c$, i.e. when squarks and sleptons are much more massive than gauginos, which generally is the limit we are interested in. Using the fact that the first and second generation squarks are approximately degenerate, and that the first and second generation squarks are usually more massive than the third generation squarks and sleptons, the ratio can be further approximated

$$\frac{C_{1jk3}^{(\overline{ud})(d\nu)}}{C_{1jk3}^{(ud)(d\nu)}} \approx \frac{\mu_R}{M_{wino}} \frac{(m_{squark}^{1,2})^2 \log(m_{\tilde{u}_{3R}}^2/m_{\tilde{e}_{3R}}^2)}{m_{\tilde{u}_{3R}}^2 - m_{\tilde{e}_{3R}}^2} \frac{\lambda_\tau \lambda_t (V_{KM})_{3k} \hat{c}_{ud}^* [1j \hat{c}_{ue}^* 3]^3}{g_2^2 (V_{KM})_{i'j} (V_{KM}^\dagger)_{j'1} \hat{c}_{qq}^{i'j'} \hat{c}_{ql}^{k]3} + g_2^2 (V_{KM})_{k'k} \hat{c}_{qq} [1j \hat{c}_{ql}^{k'}]^3} \quad (6)$$

where $m_{squark}^{1,2}$ is the mass of the first and second generation squarks.

Several factors contribute to the fact that this ratio is often greater than one. Since the third generation squarks and sleptons are lighter than the first and second generation squarks, the ratio is significantly enhanced by the factor

$(m_{\text{squark}}^{1,2})^2 \log(m_{\tilde{u}_{3R}}^2/m_{\tilde{e}_{3R}}^2)/(m_{\tilde{u}_{3R}}^2 - m_{\tilde{e}_{3R}}^2) \approx (m_{\text{squark}}^{1,2})^2/(\max(m_{\tilde{u}_{3R}}, m_{\tilde{e}_{3R}}))^2$.
Second, the ratio

$$\frac{\lambda_\tau \lambda_t (V_{KM})_{3k} \hat{c}_{ud}^* [1j \hat{c}_{ue}^* 3]_3}{g_2^2 (V_{KM})_{i'j} (V_{KM}^\dagger)_{j'1} \hat{c}_{qq}^{i'[j' \hat{c}_{ql}^k]_3} + g_2^2 (V_{KM})_{k'k} \hat{c}_{qq} [1j \hat{c}_{ql}^{k'}]_3} \quad (7)$$

is itself typically of order unity for many values of the GUT scale initial parameters. Note, this ratio is greatly enhanced in the regime of large $\tan \beta$ considered in this paper.

Finally, the ratio μ_R/M_{wino} plays a critical role in whether the LLRR operators dominate over LLLL operators in the third generation and whether the third generation anti-neutrino dominates over the second-generation. Comparing Tables A4, A5A, A5B, B4, B5A, and B5B with Tables A6 and B6, we see that there is a direct correlation between $\mu_R/m_{1/2}$ and the dominance of the third generation LLRR operators. When $\mu_R/m_{1/2}$ is small, the third generation LLRR operators can be suppressed. Moreover, because the third generation LLRR operators are suppressed when $\mu_R/m_{1/2}$ is small, the second generation anti-neutrino contributes more significantly than the third when $\mu_R/m_{1/2}$ is small.⁷ In particular, in runs I and II of the A and B tables, $\mu_R/m_{1/2}$ is small ($\sim .3$) while in runs III(1), III(2), and III(3), $\mu_R/m_{1/2}$ is near 1 or greater, and $\mu_R/m_{1/2}$ increases as one goes from run III(1) to run III(2) to run III(3). As a result, looking at the tau anti-neutrino columns of Tables A4 and B4, we see that, for any particular model, the entries of those columns for runs I and II are smaller than they are for runs III(1), III(2), and III(3), and that the entries in those columns increase steadily in going from run III(1) to III(2) to III(3). Similarly, looking at the 3rd columns of Tables A5A, A5B, B5A, and B5B, we see that the LLLL operators of the second generation anti-neutrino are fairly significant to the overall decay rate in runs I and II, while they are not quite as significant in runs III(1), III(2), and III(3), and that the significance of the LLLL operators of the second generation anti-neutrino continually decreases in going from run III(1) to III(2) to III(3).

For the first and second generation anti-neutrinos, on the other hand, the LLRR operators are negligible because they are suppressed in comparison to the LLLL operators by the up and charm Yukawa couplings, respectively. Thus, the entries in the electron and muon anti-neutrino columns of Tables A4 and B4 are fairly small, and the entries in columns 2 and 4 of Tables A5A, A5B, B5A, and B5B are fairly small. In comparison, the second generation anti-neutrino LLLL operator is the most significant of the LLLL operators, but the third generation LLLL operator is not negligible in comparison to the second generation LLLL operator. (See columns 1, 3, and 5 of Tables A5A, A5B, B5A, and B5B.)

⁷Arnowitz, et al. observed that LLRR operators can be significant to nucleon decay rates under certain circumstances in ref. [20].

5.3 $p \rightarrow \pi^+\bar{\nu}$ vs. $p \rightarrow K^+\bar{\nu}$

Secondly, we see that under certain circumstances, the decay $p \rightarrow \pi^+\bar{\nu}$ dominates over $K^+\bar{\nu}$ when the \mathcal{O}_{13} operator is included in model 4(c). When the third generation anti-neutrino dominates over the other generations, we have the approximate result

$$\begin{aligned} \frac{\Gamma(p \rightarrow \pi^+\bar{\nu})}{\Gamma(p \rightarrow K^+\bar{\nu})} &\approx 3.9 \frac{|(V_{KM})_{31}\hat{c}_{ud}^{* [11}\hat{c}_{ue}^* 3]3}|^2}{|.28(V_{KM})_{31}\hat{c}_{ud}^{* [12}\hat{c}_{ue}^* 3]3 + (V_{KM})_{32}\hat{c}_{ud}^{* [11}\hat{c}_{ue}^* 3]3}|^2} \\ &= 3.9 \left| \frac{(V_{KM})_{31}}{(V_{KM})_{32}} \right|^2 \frac{|\hat{c}_{ud}^{* [11}\hat{c}_{ue}^* 3]3}|^2}{|.28\frac{(V_{KM})_{31}}{(V_{KM})_{32}}\hat{c}_{ud}^{* [12}\hat{c}_{ue}^* 3]3 + \hat{c}_{ud}^{* [11}\hat{c}_{ue}^* 3]3}|^2} \end{aligned} \quad (8)$$

In Appendix 4, we show that $|(V_{KM})_{31}| \equiv |V_{td}|$ increases when the \mathcal{O}_{13} operator is included. The increase in the ratio of the rate of $p \rightarrow \pi^+\bar{\nu}$ versus $p \rightarrow K^+\bar{\nu}$ when the \mathcal{O}_{13} operator is included can be attributed in large part to this increase in $|V_{td}|$, since eqn. 8 contains a multiplicative factor of $|V_{td}/V_{ts}|^2$. This increase is further enhanced by the fact that $(V_{KM})_{31}\hat{c}_{ud}^{* [12}\hat{c}_{ue}^* 3]3$ has roughly the opposite sign of $(V_{KM})_{32}\hat{c}_{ud}^{* [11}\hat{c}_{ue}^* 3]3$, and hence increasing $|V_{td}|$ decreases the denominator in eqn. 8. Thus, the addition of the \mathcal{O}_{13} operator in model 4(c) increases the ratio of the $p \rightarrow \pi^+\bar{\nu}$ decay rate to $p \rightarrow K^+\bar{\nu}$, *provided* that the third generation anti-neutrino dominates.

Whether the third generation dominates over the second depends on the ratio of $\mu_R/m_{1/2}$. Thus, $p \rightarrow \pi^+\bar{\nu}$ will be larger than $p \rightarrow K^+\bar{\nu}$ if the \mathcal{O}_{13} operator is included and $\mu_R/m_{1/2}$ is not much smaller than one. Thus, in runs III(1), III(2), and III(3) of Table A1, $\mu_R/m_{1/2}$ is approximately one or bigger, and as a result the third generation anti-neutrino dominates the rate of decay, and the ratio of the rate of decay into $\pi^+\bar{\nu}$ versus the rate of decay into $K^+\bar{\nu}$ is significantly enhanced in comparison to the runs without the \mathcal{O}_{13} operator in Table B1. On the other hand, in runs I and II, $\mu_R/m_{1/2}$ is small, and as a result, the second generation dominates and the ratio of the rate of decay into $\pi^+\bar{\nu}$ versus $K^+\bar{\nu}$ remains near what it was without the \mathcal{O}_{13} operator.

5.4 “Generic” SU(5) vs Large $\tan\beta$ SO(10) models

5.4.1 $n \rightarrow \pi^0\bar{\nu}$ vs. $n \rightarrow \eta\bar{\nu}$

Furthermore, the tables of the previous section show some important differences between the nucleon decay predictions for our SO(10) model versus the predictions of a generic SUSY minimal SU(5) model. Because the effective color triplet Higgs mass is constrained to be lower than around 10^{17} GeV in SUSY minimal SU(5) [4], and because the lifetimes of the nucleons are proportional

to $\sin^2 2\beta$ [21, 20, 4], minimal SU(5) models use small $\tan\beta$ to be consistent with the experimental limits on proton decay. When $\tan\beta$ is small, LLRR operators can often be neglected. When LLRR operators are negligible, the ratio $\Gamma(n \rightarrow \pi^0 \bar{\nu})/\Gamma(n \rightarrow \eta \bar{\nu})$ just depends on chiral Lagrangian factors.

$$\begin{aligned} \frac{\Gamma(n \rightarrow \pi^0 \bar{\nu})}{\Gamma(n \rightarrow \eta \bar{\nu})} &\approx 2.8 \frac{\sum_i \left| \beta C^{(ud)}(d\nu_i) + \alpha C^{(\bar{u}\bar{d})}(d\nu_i) \right|^2}{\sum_i \left| \beta C^{(ud)}(d\nu_i) - .140\alpha C^{(\bar{u}\bar{d})}(d\nu_i) \right|^2} \\ &\approx 2.8 \end{aligned} \quad (9)$$

In contrast, when $\tan\beta$ is large, LLRR operators are not negligible. The contribution of LLRR operators to $n \rightarrow \eta \bar{\nu}$ is significantly suppressed in comparison to its contribution to $n \rightarrow \pi^0 \bar{\nu}$ by chiral Lagrangian factors. Hence, looking at Tables A1B and B1B, the rate of $n \rightarrow \pi^0 \bar{\nu}$ can be anywhere from 2.9 to over 100 times larger than the rate of $n \rightarrow \eta \bar{\nu}$, depending on whether the third generation LLRR operators or the second generation LLLL operators dominate.

5.4.2 $n \rightarrow K^0 \bar{\nu}$ vs. $p \rightarrow K^+ \bar{\nu}$

Secondly, the ratio $\Gamma(n \rightarrow K^0 \bar{\nu})/\Gamma(p \rightarrow K^+ \bar{\nu})$ differs significantly from the generic SU(5) models. Numerically,

$$\frac{\Gamma(n \rightarrow K^0 \bar{\nu})}{\Gamma(p \rightarrow K^+ \bar{\nu})} \approx \left| \frac{\beta(1.14C^{(us)}(d\nu_i) + 1.58C^{(ud)}(s\nu_i)) + \alpha(-.86C^{(\bar{u}\bar{s})}(d\nu_i) + 1.58C^{(\bar{u}\bar{d})}(s\nu_i))}{\beta(.44C^{(us)}(d\nu_i) + 1.58C^{(ud)}(s\nu_i)) + \alpha(.44C^{(\bar{u}\bar{s})}(d\nu_i) + 1.58C^{(\bar{u}\bar{d})}(s\nu_i))} \right|^2 \quad (10)$$

In the minimal SU(5) model, the $C^{(us)}(d\nu_i)$ operator is approximately equal to the $C^{(ud)}(s\nu_i)$ [21, 20, 4], and, since LLRR operators are often negligible, $\Gamma(n \rightarrow K^0 \bar{\nu})/\Gamma(p \rightarrow K^+ \bar{\nu}) \approx 1.8$. [4]. However, in our SO(10) model, LLRR operators tend to dominate. Not only are the chiral Lagrangian factors different when the LLRR operators dominate, but $C^{(\bar{u}\bar{s})}(d\nu_i)$ tends to point in the *opposite* direction as $C^{(\bar{u}\bar{d})}(s\nu_i)$. Hence, $\Gamma(n \rightarrow K^0 \bar{\nu})/\Gamma(p \rightarrow K^+ \bar{\nu})$ is much larger than its value in the minimal SU(5) models. Indeed, $n \rightarrow K^0 \bar{\nu}$ can be over 18 times bigger than $p \rightarrow K^+ \bar{\nu}$.

Also noteworthy is the fact that when LLRR operators dominate, $\Gamma(n \rightarrow K^0 \bar{\nu})/\Gamma(p \rightarrow K^+ \bar{\nu})$ is significantly higher when the \mathcal{O}_{13} operator is included in comparison to when it is not. (For example, in run III(3) $\Gamma(n \rightarrow K^0 \bar{\nu})/\Gamma(p \rightarrow K^+ \bar{\nu})$ is 18.1 with the \mathcal{O}_{13} operator included while it is no greater than 4.5 for run III(3) without the \mathcal{O}_{13} operator.) Much of the enhancement can be explained by the fact that $|V_{td}|$ is larger when the \mathcal{O}_{13} operator is included. When LLRR operators dominate,

$$\frac{\Gamma(n \rightarrow K^0 \bar{\nu})}{\Gamma(p \rightarrow K^+ \bar{\nu})} \approx \left| \frac{-.86C^{(\bar{u}\bar{s})}(d\nu_i) + 1.58C^{(\bar{u}\bar{d})}(s\nu_i)}{.44C^{(\bar{u}\bar{s})}(d\nu_i) + 1.58C^{(\bar{u}\bar{d})}(s\nu_i)} \right|^2 \quad (11)$$

Plugging eqn. 3 into this formula, this becomes

$$\frac{\Gamma(n \rightarrow K^0 \bar{\nu})}{\Gamma(p \rightarrow K^+ \bar{\nu})} \approx \left| \frac{-0.86(V_{KM})_{31} \hat{c}_{ud}^* [^{12}\hat{c}_{ue}^* 3]_3 + 1.58(V_{KM})_{32} \hat{c}_{ud}^* [^{11}\hat{c}_{ue}^* 3]_3}{.44(V_{KM})_{31} \hat{c}_{ud}^* [^{12}\hat{c}_{ue}^* 3]_3 + 1.58(V_{KM})_{32} \hat{c}_{ud}^* [^{11}\hat{c}_{ue}^* 3]_3} \right|^2 \quad (12)$$

Since $(V_{KM})_{31} \hat{c}_{ud}^* [^{12}\hat{c}_{ue}^* 3]_3$ tends to have the opposite sign as $(V_{KM})_{32} \hat{c}_{ud}^* [^{11}\hat{c}_{ue}^* 3]_3$, $\Gamma(n \rightarrow K^0 \bar{\nu})/\Gamma(p \rightarrow K^+ \bar{\nu})$ is enhanced when $|V_{td}|$ is increased.

5.5 Sensitivity to “22” Clebsch

Furthermore, by looking at Tables B1 through B6, we can determine how sensitive nucleon decay rate predictions are on the Clebsches that enter into the c_{qq} , c_{ql} , c_{ud} , and c_{ue} matrices. For each of the five runs of Tables B1 through B6, the *only* difference between the versions a through f in each run are the y_{qq} , y_{ql} , y_{ud} and y_{ue} Clebsches of Table 1 that enter into the c_{qq} , c_{ql} , c_{ud} , and c_{ue} matrices. We see that the overall rate of decay is quite sensitive to the different choices for Clebsches. For example, with $\beta = -\alpha$, $\tau(p \rightarrow K^+ \bar{\nu})$ for run I(e) is 7 times larger than $\tau(p \rightarrow K^+ \bar{\nu})$ for run I(f). The branching ratios generally exhibit less sensitivity: $\Gamma(n \rightarrow \pi^0 \bar{\nu})/\Gamma(n \rightarrow K^0 \bar{\nu})$ exhibits virtually no sensitivity and $\Gamma(p \rightarrow \pi^+ \bar{\nu})/\Gamma(p \rightarrow K^+ \bar{\nu})$ exhibits relatively mild sensitivity. However, branching ratios into less dominant decay modes can at certain times exhibit high sensitivity. For example, with $\beta = -\alpha$, $\Gamma(n \rightarrow \eta \bar{\nu})/\Gamma(n \rightarrow K^0 \bar{\nu})$ is over 12 times larger for run I(f) than it is for run I(c).

5.6 Gluino vs. Chargino contributions

It can also be seen that the contributions of gluinos to the rate of nucleon decay is often not negligible. Indeed, in several examples, excluding the gluinos’ contribution can lead to a decrease in the predicted rate of decay of greater than 60%, in cases where gluinos constructively interfere, or an increase in the rate of decay by over 150%, where gluinos destructively interfere.⁸ Note also that whether gluinos constructively or destructively interfere depends heavily on the phase of the chiral Lagrangian parameter $\arg(\beta/\alpha)$.

5.7 Proton decay from gauge boson exchange

Finally we note that our analysis only includes the contribution to nucleon decay from the effective dimension 5 operators resulting from colored triplet Higgs exchanges. We have neglected the contribution to nucleon decay via heavy gauge boson exchange (effective dimension 6 operators). This approximation is justified in our models for the dominant decay modes. For example, in order to

⁸Goto, et al. observed that gluino loops can be important in the minimal SU(5) model in ref. [22].

obtain the ϵ_3 of run III(1), we can choose the vevs a_1 , a_2 , \tilde{a} , and a singlet field \mathcal{S}_4 , defined in paper I, which enter into the $SO(10)$ breaking sector of the theory, to be 2.0×10^{16} GeV, 1.0×10^{16} GeV, 6.0×10^{16} GeV, and $.66 \times 10^{16}$ GeV, respectively, i.e. all of order M_{GUT} . Then the masses of the gauge bosons contained in $SO(10)/(SU(3) \times SU(2) \times U(1)) - X^\pm$, Q^\pm , U^\pm , and E^\pm are 3.2×10^{16} GeV, 1.2×10^{17} GeV, 1.3×10^{17} GeV, and 1.3×10^{17} GeV, respectively⁹. The decay mode which would be the most dominant if all other contributions to proton decay except the contribution due to gauge boson exchanges were neglected is $p \rightarrow \pi^0 e^+$. With the above gauge boson masses, the partial proton lifetime due to heavy gauge boson exchanges for $p \rightarrow \pi^0 e^+$ is 1.2×10^{38} yrs, corresponding to a branching ratio of order $< 10^{-4}$. Of the decay modes listed in Tables A1A and B1A, gauge exchange is competitive only with $p \rightarrow \eta \mu^+$.

Conclusions

We have shown in this paper that model 4(c) of paper I predicts nucleon decay rates consistent with all current experimental bounds, while using values of GUT parameters that give fermion masses, mixing angles, and gauge couplings in good agreement with experimental observations. Our main results can be found in Tables A1A, A1B, and A6. We conclude that our model predicts that nucleon decay is likely to be observed by SuperKAMIOKANDE or ICARUS, which are expected to probe nucleon lifetimes up to around 10^{34} yrs [23, 24], for various decay modes predicted by GUTs.

In order to avoid this conclusion one would need to make squarks and sleptons “unnaturally” heavy and beyond the reach of LHC or increase the effective color triplet Higgs mass \tilde{M}_t , which would require a supermassive Higgs doublet in the GUT desert with mass many orders of magnitude lower than the GUT scale and at least an order of magnitude lighter than any other particle getting mass around the GUT scale. Moreover, we have chosen the poorly known chiral Lagrangian parameter $|\beta|$ to be at the lowest value suggested by the data. If it could be shown that $|\beta|$ lies in the higher range of its current bounds, non-observation of nucleon decay by SuperKAMIOKANDE and ICARUS could make our model unnatural for any reasonable values of the squark and slepton masses.¹⁰ For these reasons, we believe that these models, if correct, necessarily lead to observable nucleon decay rates.

We have shown that LLRR operators are not only significant, but often dominate, nucleon decay in the large $\tan \beta$ regime – as long as $\mu_R/m_{1/2}$ is

⁹Note, the X^\pm gauge boson is the massive gauge boson from the 24 representation of $SU(5)$; Q^\pm is the gauge boson from the 10, 15, $\overline{10}$, and $\overline{15}$ representations of $SU(5)$ which is in the $(3, 2, \frac{1}{3})$ and $(\overline{3}, 2, -\frac{1}{3})$ representations of $SU(3) \times SU(2) \times U(1)$; and U^\pm and E^\pm are gauge bosons from the 10 and $\overline{10}$ representations of $SU(5)$ which are in $\{(3, 1, \frac{4}{3}), (\overline{3}, 1, -\frac{4}{3})\}$ and $\{(1, 1, -2), (1, 1, 2)\}$ representations of $SU(3) \times SU(2) \times U(1)$, respectively.

¹⁰ Recall, however, that the chiral Lagrangian approach tends to overestimate nucleon decay rates [16] and thus underestimates the lifetimes.

not very small. As a result, if nucleon decay is observed, there are two key experimental observables that may distinguish between large or small $\tan \beta$ SUSY GUTs: the ratios $\Gamma(n \rightarrow K^0 \bar{\nu})/\Gamma(p \rightarrow K^+ \bar{\nu})$ and $\Gamma(n \rightarrow \eta \bar{\nu})/\Gamma(n \rightarrow \pi^0 \bar{\nu})$. In particular, evidence for a neutron lifetime $(\frac{1}{5} - \frac{1}{20}) \times$ the proton lifetime would be a strong indication for large $\tan \beta$ SUSY GUTs. Observation of $\Gamma(n \rightarrow \eta \bar{\nu})/\Gamma(n \rightarrow \pi^0 \bar{\nu})$ significantly lower than than the predicted value when LLRR operators are negligible could also indicate large $\tan \beta$ SUSY GUTs.

We have also shown that gaugino loops cannot be neglected when calculating proton decay rates in models such as ours. In fact, neglecting gaugino loops could lead to an underestimation of the decay rates of over 60% or overestimation of over 150%.

Finally, we have studied the sensitivity of nucleon lifetime and branching ratio predictions on the “quality” of the predictions that these models make for fermion masses and mixing angles. In the models we have analyzed, the entries in the c_{qq} , c_{ql} , c_{ud} , and c_{ue} matrices are related to entries in the Y_u , Y_d , and Y_e matrices by Clebsches which depend on the version of the model being considered. As we have seen, the lifetimes and branching ratios can be quite sensitive to the choice of Clebsches — some predictions vary by nearly an order of magnitude depending on the choice of Clebsches. In models 4(a) through (f), without the \mathcal{O}_{13} operator, the different Clebsches have no effect on the predictions for fermion masses and mixing angles. Comparing models 4(a) through (f), without the \mathcal{O}_{13} operator, which is consistent with fermion masses and mixing angles at 2σ , with model 4(c), with the \mathcal{O}_{13} operator, which is consistent within 1σ , one is lead to conclude that fitting the data within 1 or 2 σ can have a significant effect on the nucleon decay predictions. Thus “predictions” for nucleon decay lifetimes and branching ratios cannot be expected to be any better than the complementary predictions for fermion masses and mixing angles.

Acknowledgments

This research was supported in part by the U.S. Department of Energy contract DOE/ER/01545-697. We would like to thank Tomáš Blažek, Marcela Carena, and Carlos Wagner for letting us use the results of work in progress on a general χ^2 analysis of fermion masses.

Appendix 1: How the Dimopoulos-Wilczek mechanism can produce $\tilde{M}_t \gg M_{GUT}$

Using the Dimopoulos-Wilczek mechanism for doublet-triplet splitting, the part of the superspace potential in our model giving doublet-triplet splitting is

$$W_{d-t} = 10_1 A_1 10_2 + 10_2^2 \mathcal{S}_*,$$

where A_1 is a 45 representation getting a vev of order M_{GUT} in the baryon minus lepton number direction, 10_1 and 10_2 are 10 representations, and \mathcal{S}_* is a singlet. The Higgs doublet and triplet mass matrices for our model are

$$M_t = \begin{matrix} & 10_1 & 10_2 \\ \begin{matrix} 10_1 \\ 10_2 \end{matrix} & \begin{pmatrix} 0 & a_1 \\ -a_1 & \mathcal{S}_* \end{pmatrix} \end{matrix} \quad (13)$$

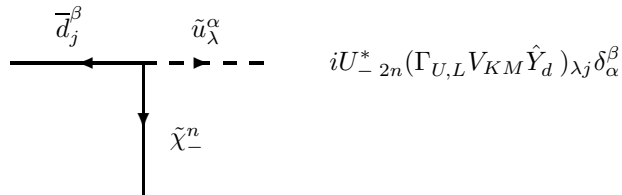
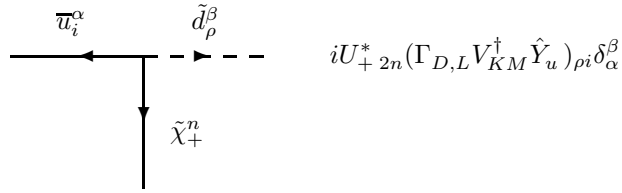
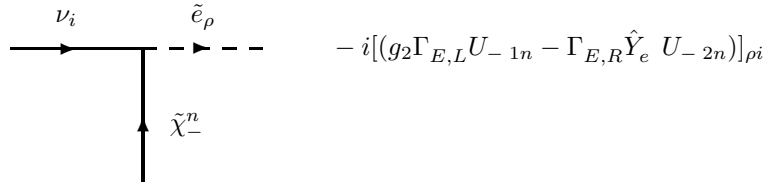
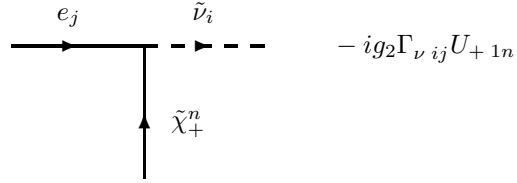
$$M_d = \begin{matrix} & 10_1 & 10_2 \\ \begin{matrix} 10_1 \\ 10_2 \end{matrix} & \begin{pmatrix} 0 & 0 \\ 0 & \mathcal{S}_* \end{pmatrix} \end{matrix} \quad (14)$$

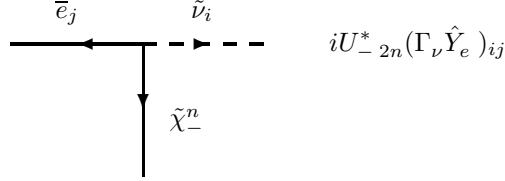
Note, the 10_1 field is the only 10 representation that couples to ordinary (Standard Model) fermions. Thus, the 10_1 contains the two Higgses of the Minimal SUSY Standard Model [MSSM], and the baryon-number violating effective operators obtained by integrating out the color triplets are proportional to $1/\tilde{M}_t \equiv (M_t^{-1})_{11} = \mathcal{S}_*/a_1^2$, the $10_1, 10_1$ entry of the inverse of the color triplet mass matrix. An effective color triplet mass of around 10^{19} GeV is obtained with a_1 around the GUT scale, and \mathcal{S}_* around 10^{13} GeV. Thus, $\tilde{M}_t \gg M_{GUT}$ means that there is an electroweak doublet several orders of magnitude lighter than the GUT scale, not that there is an actual color triplet with mass greater than M_{Planck} [25].

Appendix 2: Feynman diagrams

$$-i[(g_2 \Gamma_{U,L} U_{+1n} - \Gamma_{U,R} \hat{Y}_u U_{+2n}) V_{KM}]_{\lambda j} \delta_\beta^\alpha$$

$$-i[(g_2 \Gamma_{D,L} U_{-1n} - \Gamma_{D,R} \hat{Y}_d U_{-2n}) V_{KM}^\dagger]_{\rho i} \delta_\beta^\alpha$$





Appendix 3: Formulas for nucleon decay in terms of chiral Lagrangian factors

Using the chiral Lagrangian techniques of ref. [14], the rates of nucleon decay are the following.

$$\begin{aligned}
\Gamma(p \rightarrow K^+ \bar{\nu}_i) &= \frac{(m_p^2 - m_K^2)^2}{32\pi m_p^3 f_\pi^2} A_L^2 \left| [\beta C^{(us)(d\nu_i)} + \alpha C^{(\bar{u}s)(d\nu_i)}] \frac{2m_p}{3m_B} D \right. \\
&\quad \left. + [\beta C^{(ud)(s\nu_i)} + \alpha C^{(\bar{u}d)(s\nu_i)}] \left[1 + \frac{m_p}{3m_B} (D + 3F) \right] \right|^2 \\
\Gamma(p \rightarrow \pi^+ \bar{\nu}_i) &= \frac{m_p}{32\pi f_\pi^2} A_L^2 \left| [\beta C^{(ud)(d\nu_i)} + \alpha C^{(\bar{u}d)(d\nu_i)}] (1 + D + F) \right|^2 \\
\Gamma(p \rightarrow \eta e_i^+) &= \frac{3(m_p^2 - m_\eta^2)^2}{64\pi f_\pi^2 m_p^3} A_L^2 \left\{ \left| \beta C^{(ud)(ue_i)} \left[1 + \frac{1}{3}(3F - D) \right] - \alpha C^{(\bar{u}d)(ue_i)} \frac{1}{3} [1 - (3F - D)] \right|^2 \right. \\
&\quad \left. + \left| \beta C^{(\bar{u}d)(\bar{u}e_i)} \left[1 + \frac{1}{3}(3F - D) \right] - \alpha C^{(ud)(\bar{u}e_i)} \frac{1}{3} [1 - (3F - D)] \right|^2 \right\} \\
\Gamma(p \rightarrow K^0 e_i^+) &= \frac{(m_p^2 - m_K^2)^2}{32\pi f_\pi^2 m_p^3} A_L^2 \left\{ \left| \beta C^{(us)(ue_i)} \left[1 - \frac{m_p}{m_B} (D - F) \right] - \alpha C^{(\bar{u}s)(ue_i)} \left[1 + \frac{m_p}{m_B} (D - F) \right] \right|^2 \right. \\
&\quad \left. + \left| \beta C^{(\bar{u}s)(\bar{u}e_i)} \left[1 - \frac{m_p}{m_B} (D - F) \right] - \alpha C^{(us)(\bar{u}e_i)} \left[1 + \frac{m_p}{m_B} (D - F) \right] \right|^2 \right\} \\
\Gamma(p \rightarrow \pi^0 e_i^+) &= \frac{m_p}{64\pi f_\pi^2} A_L^2 \left\{ \left| [\beta C^{(ud)(ue_i)} + \alpha C^{(\bar{u}d)(ue_i)}] (1 + D + F) \right|^2 \right. \\
&\quad \left. + \left| [\beta C^{(\bar{u}d)(\bar{u}e_i)} + \alpha C^{(ud)(\bar{u}e_i)}] (1 + D + F) \right|^2 \right\} \\
\Gamma(n \rightarrow K^0 \bar{\nu}_i) &= \frac{(m_n^2 - m_K^2)^2}{32\pi m_n^3 f_\pi^2} A_L^2 \left| \beta C^{(us)(d\nu_i)} \left(1 - \frac{m_n}{3m_B} (D - 3F) \right) - \alpha C^{(\bar{u}s)(d\nu_i)} \left(1 + \frac{m_n}{3m_B} (D - 3F) \right) \right. \\
&\quad \left. + (\beta C^{(ud)(s\nu_i)} + \alpha C^{(\bar{u}d)(s\nu_i)}) \left(1 + \frac{m_n}{3m_B} (D + 3F) \right) \right|^2
\end{aligned}$$

$$\begin{aligned}
\Gamma(n \rightarrow \pi^0 \bar{\nu}_i) &= \frac{m_n^3}{64\pi f_\pi^2} A_L^2 \left| \beta C^{(ud)(d\nu_i)} + \alpha C^{(\bar{u}\bar{d})(d\nu_i)} \right|^2 (1 + D + F)^2 \\
\Gamma(n \rightarrow \eta \bar{\nu}_i) &= \frac{3(m_n^2 - m_\eta^2)^2}{64\pi m_n^3 f_\pi^2} A_L^2 \left| \beta C^{(ud)(d\nu_i)} \left(1 + \frac{1}{3}(3F - D)\right) - \alpha C^{(\bar{u}\bar{d})(d\nu_i)} \frac{1}{3}(1 + D - 3F) \right|^2 \\
\Gamma(n \rightarrow \pi^- e_i^+) &= \frac{m_n}{32\pi f_\pi^2} A_L^2 \left\{ \left| \beta C^{(ud)(ue_i)} + \alpha C^{(\bar{u}\bar{d})(ue_i)} \right|^2 + \left| \beta C^{(\bar{u}\bar{d})(\bar{u}e_i)} + \alpha C^{(ud)(\bar{u}e_i)} \right|^2 \right\} (1 + D + F)^2
\end{aligned}$$

where m_B is an average Baryon mass satisfying $m_B \approx m_\Sigma \approx m_\Lambda$ and all other notation follows [14]¹¹. Here, all coefficients of four-fermion operators are evaluated at M_Z . A_L takes into account renormalization from M_Z to 1 GeV, and is approximately equal to .22. [13]. These formulas reduce to the chiral Lagrangian formulas given in ref. [4] for $\beta \neq 0$ when $\alpha = 0$. In the calculations, we take $D = .81$, $F = .44$ [4], and $f_\pi = 139$ MeV [14].

Appendix 4: Why $|V_{td}|$ increases when the \mathcal{O}_{13} is included in model 4(c)

It can be seen that our Y_d and Y_e matrices, which have the general form,

$$\begin{pmatrix} 0 & zC & uDe^{i\delta} \\ zC & yEe^{i\phi} & xB \\ u'De^{i\delta} & x'B & A \end{pmatrix}$$

with $C, D \ll B, E \ll A$, can be diagonalized by multiplying the matrices on the left and right by matrices S and T , respectively, where

$$\begin{aligned}
S &\approx \begin{pmatrix} 1 & -(zC - \frac{x'uBD}{A}e^{i\delta})\frac{e^{-i\phi}}{yE} & -\frac{uDe^{i\delta}}{A} + \frac{xBe^{-i\phi}}{yEA}(zC - \frac{x'uBD}{A}e^{i\delta}) \\ (zC - \frac{x'uBD}{A}e^{-i\delta})\frac{e^{i\phi}}{yE} & 1 & -\frac{xB}{A} \\ \frac{uDe^{-i\delta}}{A} & \frac{x'B}{A} & 1 \end{pmatrix} \\
T &\approx \begin{pmatrix} 1 & (zC - \frac{xu'BD}{A}e^{-i\delta})\frac{e^{i\phi}}{yE} & \frac{u'De^{-i\delta}}{A} \\ -(zC - \frac{xu'BD}{A}e^{i\delta})\frac{e^{-i\phi}}{yE} & 1 & \frac{x'B}{A} \\ -\frac{u'De^{i\delta}}{A} + \frac{x'B e^{-i\phi}}{yEA}(zC - \frac{xu'BD}{A}e^{i\delta}) & -\frac{x'B}{A} & 1 \end{pmatrix}
\end{aligned}$$

Our Y_u matrix, which has the general form

$$\begin{pmatrix} 0 & zC & uDe^{i\delta} \\ zC & 0 & xB \\ u'De^{i\delta} & x'B & A \end{pmatrix}$$

¹¹ $C_{ijkl}^{(ud)(d\nu)} = C_{ijkl}^{(ud)(d\nu)[G]} + C_{ijkl}^{(ud)(d\nu)[W]}$, etc.

with $C, D \ll B, E \ll A$ and $C \ll xx'B^2/A$, is diagonalized by the S and T matrices

$$S \approx \begin{pmatrix} 1 & \frac{A}{xx'B^2}(zC - \frac{x'uBD}{A}e^{i\delta}) & -\frac{zC}{x'B} \\ -\frac{A}{xx'B^2}(zC - \frac{x'uBD}{A}e^{-i\delta}) & 1 & -\frac{x'B}{A} \\ \frac{uD}{A}e^{-i\delta} & \frac{x'B}{A} & 1 \end{pmatrix}$$

$$T \approx \begin{pmatrix} 1 & -\frac{A}{xx'B^2}(zC - \frac{x'uBD}{A}e^{-i\delta}) & \frac{u'D}{A}e^{-i\delta} \\ \frac{A}{xx'B^2}(zC - \frac{x'uBD}{A}e^{i\delta}) & 1 & \frac{x'B}{A} \\ -\frac{zC}{xB} & -\frac{x'B}{A} & 1 \end{pmatrix}$$

Therefore, at M_{GUT}

$$V_{td} \approx \frac{D}{A}e^{i\delta}(u_u - u_d) + \frac{BC}{AE}e^{-i\phi}\frac{z_d}{y_d}(x_d - x_u) + \left(\frac{B}{A}\right)^2\frac{D}{E}\frac{(x_u - x_d)x'_d u_d}{y_d}e^{i(\delta-\phi)}$$

$$= -2\frac{D}{A}e^{i\delta} - 12\frac{BC}{AE}e^{-i\phi} + \frac{16}{243}\left(\frac{B}{A}\right)^2\frac{D}{E}e^{i(\delta-\phi)}$$

$$\approx -12e^{-i\phi}\left(\frac{BC}{AE} + \frac{1}{6}\frac{D}{A}e^{i(\delta+\phi)}\right) \quad (15)$$

Since $\delta + \phi \approx 30^\circ$, the $D e^{i(\delta+\phi)}/(6A)$ term will increase $|V_{td}|$ provided that the $BC/(AE)$ term does not decrease too much when the \mathcal{O}_{13} operator is included.

What effect does the \mathcal{O}_{13} operator have on the A , B , C , and E parameters? The A parameter will not be affected at all because A is fixed purely by the third generation masses m_b and m_τ [7]. Moreover, the first generation Yukawa coupling λ_e of the Y_e matrix is approximately equal to

$$\frac{243}{E}\left|C^2 - \frac{109}{27}CD\frac{B}{A}e^{i\delta}\right| \quad (16)$$

at M_{GUT} . Since δ is typically close to 2π , the term of the absolute value linear in D decreases the eigenvalue. Therefore, C must be increased to compensate for the \mathcal{O}_{13} operator.

On the other hand, when B is evaluated by using the global χ^2 analysis of ref. [9], B actually decreases when the \mathcal{O}_{13} operator is included. It will be shown in ref. [9] that when a global χ^2 analysis is done, B_K , the bag constant which comes into the theoretical formula for the experimental observable ϵ_K measuring CP violation, and $|V_{cb}|$ come out too high; and $|V_{ub}/V_{cb}|$ comes out too low, in comparison with their experimental measurements, for model 4 without an \mathcal{O}_{13} operator. Since $V_{cb} \approx \zeta|x_d - x_u|B/A$ where ζ is a renormalization group factor, this means that B is too high. It will also be shown in ref. [9] that unless an \mathcal{O}_{13} operator is included, V_{cb} and V_{ub}/V_{cb} cannot be corrected by

changing the parameters without further increasing B_K , which is already too high. Furthermore, B and E are related by the equation

$$|3AEe^{i\phi} - B^2| \approx \lambda_\mu \lambda_\tau.$$

Since $\text{Re } \phi < 0$, E is lower when the \mathcal{O}_{13} operator is not included because B is higher than it should be.

However, when the \mathcal{O}_{13} operator of paper I is added to model 4(c), it is possible to lower B to bring it in line with the experimental value for $|V_{cb}|$ while simultaneously having reasonable values for B_K as well as for the other observables [9]. The net effect of including the \mathcal{O}_{13} operator to model 4(c) is that B is typically decreased by $\sim 10\%$, E is increased by $\sim 18\%$, and C is increased by $\sim 25\%$. Therefore, $BC/(AE)$ actually decreases slightly ($\sim 3\%$). However, the decrease in that term is more than compensated for by the increase in $|V_{td}|$ due to the $\frac{D}{\delta A}e^{i(\delta+\phi)}$ term. The net result of the inclusion of the \mathcal{O}_{13} operator is an increase in $|V_{td}|$ typically of $\sim 11\%$.

References

- [1] M. Gell-Mann, P. Ramond and R. Slansky, *Rev. Mod. Phys.* **50** 721 (1972); H. Georgi and S. Glashow, *Phys. Rev. Lett.* **32** 438 (1974); J. Pati and A. Salam, *Phys. Rev.* **D8** 1240 (1973)
- [2] S. Weinberg, *Phys. Rev.* **D26**, 287 (1982); N. Sakai and T Yanagida, *Nucl. Phys.* **B197**, 533 (1982).
- [3] S. Dimopoulos, S. Raby and F. Wilczek, *Phys. Lett.* **112B** 133 (1982); J. Ellis, D.V. Nanopoulos and S. Rudaz, *Nucl. Phys.* **B202** 43 (1982). For recent analyses, see R. Arnowitt and P. Nath, *Phys. Rev.* **D49** 1479 (1994); J. Hisano, H. Murayama, and T. Yanagida, *Nucl. Phys.* **B402** 46 (1993); P. Langacker, “Proton Decay,” (LANL hep-ph/9210238) talk given at The Benjamin Franklin Symposium in Celebration of the Discovery of the Neutrino, Philadelphia, PA, 29 Apr - 1 May (1992); and T. Goto, T. Nihei, and J. Arafune, *Phys. Rev.* **D52** 505 (1995).
- [4] J. Hisano, H. Murayama, and T. Yanagida, *Nuc. Phys.* **B402** 46 (1993)
- [5] J. Bagger, K. Matchev, and D. Pierce, *Phys. Lett.* **B348** 443 (1995).
- [6] V. Lucas and S. Raby, *Phys. Rev.* **D54** 2261 (1996).
- [7] G. Anderson, S. Dimopoulos, L.J. Hall, S. Raby and G. Starkman, *Phys. Rev.* **D49** 3660 (1994).
- [8] S. Dimopoulos and F. Wilczek, in *The Unity of the Fundamental Interactions*, Proceedings of the 19th Course of the International School of Subnuclear Physics, Erice, Italy, 1981, edited by A. Zichichi (Plenum, New York, 1983).
- [9] T. Blažek, M. Carena, S. Raby and C. Wagner, A Global χ^2 Analysis of Electroweak Data (including Fermion Masses and Mixing Angles) in SO(10) SUSY GUTs, OHSTPY-HEP-T-96-014 (LANL hep-ph/9608273)(1996); and paper in preparation.
- [10] S. Bertolini, F. Borzumati, A. Masiero, and G. Ridolfi, *Nucl. Phys.* **B353** 591 (1991).
- [11] J. Ellis, J.S. Hagelin, D.V. Nanopoulos, and K. Tamvakis, *Phys. Lett.* **124B** 484 (1983); V.M. Belyaev and M.I. Vysotsky, *Phys. Lett.* **127B** 275 (1983); S. Chadha, G.D. Coughlan, M. Daniel, and G.G. Ross, *Phys. Lett.* **149B** 477 (1984).
- [12] S.P. Martin and M.T. Vaughn, *Phys Rev.* **D50** 2282 (1994).
- [13] J. Ellis, D.V. Nanopoulos, and S. Rudaz, *Nuc. Phys.* **B202** 43 (1982).

- [14] M. Claudson, M. Wise, L.H. Hall, *Nuc. Phys.* **B195** 297 (1982); S. Chadha and M. Daniel, *Nuc. Phys.* **B229** 105 (1983).
- [15] S.J. Brodsky, J. Ellis, J.S. Hagelin, C. Sachradja, *Nucl. Phys.* **B238** 561 (1984).
- [16] M.B. Gavela, S.F. King, C.T. Sachrajda, G. Martinelli, M.L. Paciello, and B. Taglienti, *Nucl. Phys.* **B312** 269 (1989).
- [17] M.B. Gavela, S.F. King, C.T. Sachrajda, G. Martinelli, M.L. Paciello, and B. Taglienti, *Nucl. Phys.* **B312** 269 (1989); Y. Hara, S. Itoh, Y. Iwasaki, and T. Yoshie, *Phys. Rev.* **D34** 3399 (1986); S.J. Brodsky, J. Ellis, J.S. Hagelin, C. Sachradja, *Nucl. Phys.* **B238** 561 (1984).
- [18] Y. Hara, S. Itoh, Y. Iwasaki, and T. Yoshie, *Phys. Rev.* **D34** 3399 (1986).
- [19] The Particle Data Group, *Phys. Rev.* **D54** 1, et seq. (1996).
- [20] R. Arnowitt, A.H. Chamseddine, and P. Nath, *Nucl. Phys.* **B202** 43 (1985).
- [21] R. Arnowitt and P. Nath, *Phys. Rev.* **D38** 1479 (1988).
- [22] T. Goto, T. Nihei, and J. Arafune, *Phys. Rev.* **D52** 505 (1995).
- [23] Y. Totsuka, *Proc. of Intern Symposium on Underground Physics Experiments*, Institute for Cosmic Ray Research report, ICRR-227-90-20 (1990).
- [24] D.B. Cline, *Nucl. Instruments and Methods in Physics Research* **A327** 178 (1993).
- [25] These results were also discussed by K.S. Babu and S.M. Barr, *Phys. Rev.* **D48** 5354 (1993).